PHYSICAL MEASUREMENTS OF RODENT URINE

FOR THE

ADVANCED ANIMAL HABITAT - CENTRIFUGE (AAH-C) PROJECT

John P. Kizito, Ph.D.

Jeffrey Allen, Ph.D.

Karen L. Barlow

The National Center for Microgravity Research
21000 Brookpark Road, MS 110-3
Cleveland, Ohio 44135
216-433-2275
fax: 216-433-3793
email: John.P.Kizito@grc.nasa.gov

January - June 2001

A. RECORD OF REVIEW AND APPROVAL

Prepared By: _____ Date_____
Karen L. Barlow
NCMR Lab Assistant

Approved By: _____ Date_____
Jeff Allen
NCMR Staff Scientist

Approved By: _____ Date_____
John P. Kizito
NCMR Staff Scientist

B. REVISION HISTORY

REV	DATE	PAGES AFFECTED	INSTRUCTIONS/REMARKS

C. PROPRIETARY DOCUMENT

This document contains certain data that constitutes intellectual property of STAR-SHOT and is proprietary in nature. Authorized copies of this document are controlled, distributed, and recorded through the STAR-SHOT Document Management System. Distribution and review of this document outside of this management system is not authorized unless written permission is requested and granted from the STAR-SHOT Project Manager.

TABLE OF CONTENTS

1. EXECUTIVE SUMMARY

The density, viscosity, and surface tension of rat and mouse urine were explored using the methods described in this report. The following results were acquired at room temperature (23°C). The density of female rat urine was 1.002 g/mL, while the male rat urine averaged 0.967 g/mL. The density of male mouse urine was 1.050 g/mL, while the female mouse urine was slightly less dense with an average of 1.03 g/mL. The kinematic viscosity and surface tension of rat urine were 0.99 cSt and 36.47 dynes/cm, respectively. Both properties decreased with increasing temperature. The kinematic viscosity and surface tension of mouse urine were 1.12 cSt and 46.68 dynes/cm, respectively, and while the viscosity decreased with increasing temperature, the surface tension remained constant. The contact angles of rat and mouse urines on stainless steel were 45 and 47 degrees, respectively. On earth, hysteresis[a] is a function of the volume of a droplet of urine. For very small volumes, there was no hysteresis when the substrate was rotated. When a Wilhelmy plate was immersed in a container of urine, the force measured exhibited hysteresis when the capillary number[b] is of the order 10^{-4}. The evaporation of mouse urine was linear at room temperature for the duration measured.

From our results, we conclude that different strategies must be used for the removal of mouse urine in comparison to rat urine (an explanation will be given in section 6). Application of capillary transport techniques to the mouse urine must be performed as soon as the urine exits the animal. More studies will be needed to determine the relevant time scales to describe the window of opportunity.

2. INTRODUCTION

To preserve the health of the rodent subjects as well as to prevent contamination of the video camera and lens system of the AAH-C, it will be necessary to determine a method of urine removal. Based on preliminary studies, wet rodents develop hypothermia, and camera lenses are fouled in a matter of days.[1] As a first step toward eliminating this problem, physical property measurements were performed on urine samples in order to predict how the fluid might behave in microgravity.

Samples of urine collected from Sprague Dawley rats and ICR strain mice were sent from STAR Enterprises, Inc. and the physical aspects including density, surface tension, and viscosity, as well as other characteristics related to these basic properties were analyzed. These properties are directly related to the transport of the urine when contacting cage walls or mesh of the rodent habitats and with this data it will be possible to model the behavior of the urine in order to find satisfactory techniques of waste handling.

---

[a] Hysteresis represents a history dependence of physical parameters on a path: Forward outputs of the system do not equal their reverse resulting in a non-linear representation of the system. See section 7 for more details.

[b] $Ca = \frac{\eta u}{\sigma}$ where η is the absolute viscosity, u is the relative velocity between the fluid and the substrate, and σ is the surface tension.

3. URINE FILTRATION & STORAGE

3.1. Methods and Materials

Ideally, fresh samples of urine would have been used for each experiment. However, since the supply of urine was scarce, recycling and refrigeration of the urine was necessary. The thought of designing synthetic urine was proposed early in the project, but this task was proved too difficult without proper chemical analysis of the urine, and the effort was abandoned. Therefore, many of the results were supplied from samples that may have undergone, to some extent, evaporation and oxidation. To monitor degradation of the urine, the pH of each sample was collected throughout its use and samples that exceeded a pH of 7.0 were discarded.

There was a high degree of contamination with food, feces and drinking water with batch #10601 due to the apparatus with which the urine was collected. Subsequent samples were collected with a different method and then filtered with a Millepore Sterivac® vacuum-driven filter (Fisher cat.#SKGP M10 RJ). See Appendix A for more detail on urine collection methods.

4. DENSITY

4.1. Methods and Materials

A high precision balance (Thomas Scientific T200S) was used to measure the mass of all liquids. The mass of a 25mL beaker was first recorded and 1.00 mL of liquid was measured using one of the following pipette methods. The total mass of the container and the liquid was recorded and the mass of the liquid was calculated and plotted versus the cumulative volume of liquid. The density was found by determining the slope of the line.

4.1.1. *Analog Pipette*

A Kimax-51® glass pipette was used with a rubber bulb attachment to measure 1.00 mL of liquid. The meniscus of the liquid was measured at eye level, and the liquid was dispensed into the 25mL beaker.

4.1.2. *Digital Pipette*

A Labsystems Finnpipette® (1-5mL) digital pipette with disposable tip was used to measure and dispense, according to the manufacturer's instructions, 1.00 mL of liquid into the beaker on the balance.

With the analysis of liquids with known densities, we concluded this method provides an inexpensive, repeatable, and easy way of measuring density accurately. The method using the digital pipette was preferred, as it decreased the probability of human error. For this reason, only figure 4 in the following section was generated using the analog pipette.

4.2. Results

4.2.1. *Water and Calibration*

Deionized ultra-filtered water (Fisher #W2-20) was used to calibrate the digital pipette. The resistivity of the water was tested with a Corning Checkmate II® conductivity meter to assure its purity. The density for the water was determined to be 1.00 g/mL as shown in the mass versus volume plot (see figure 1). Periodically, the pipette was cleaned according to the manufacturer's recommendations. The pipette was subsequently re-calibrated using D.I.U.F water. The digital pipette was adjusted until the density reading of the D.I.U.F water was as close to 1.00 g/mL as possible. The resulting density graph is shown in figure 2.

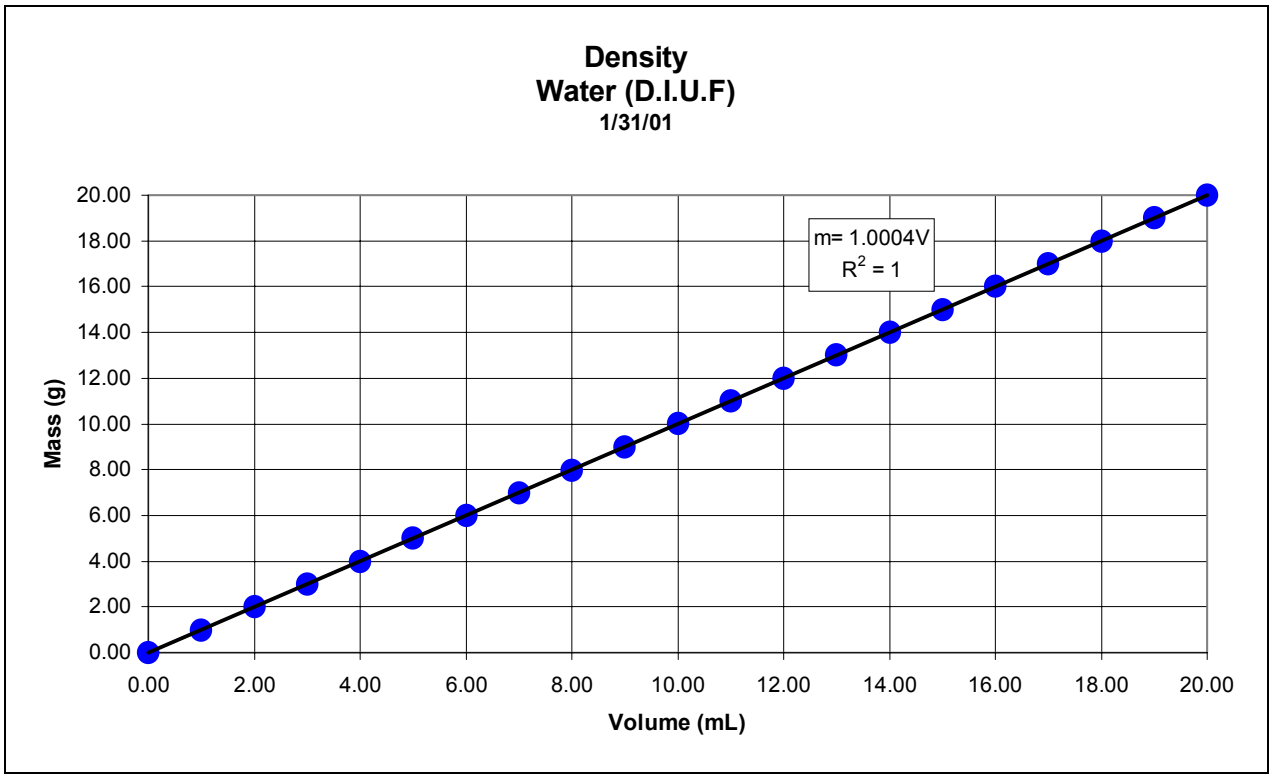

Figure 1: Calibration Plot. Density of D.I.U.F water.

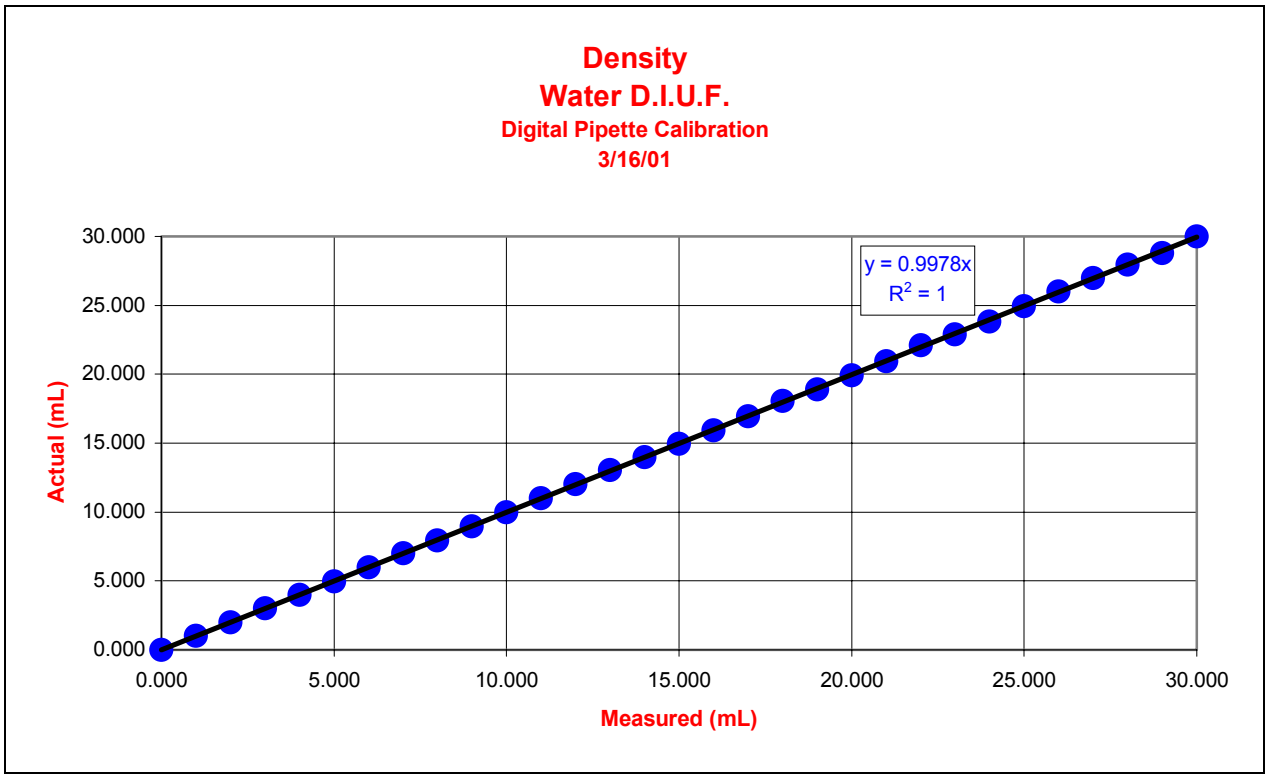

Figure 2: **Re-calibration of the digital pipette after cleaning.**

4.2.2. *Ethanol*

The densities of ethanol and water were measured in order to determine whether the above protocol was acceptable. The graph in figure 3 proves the density acquired by this method is comparable to the value 0.7893 g/mL listed in the *CRC Handbook of Chemistry and Physics*.

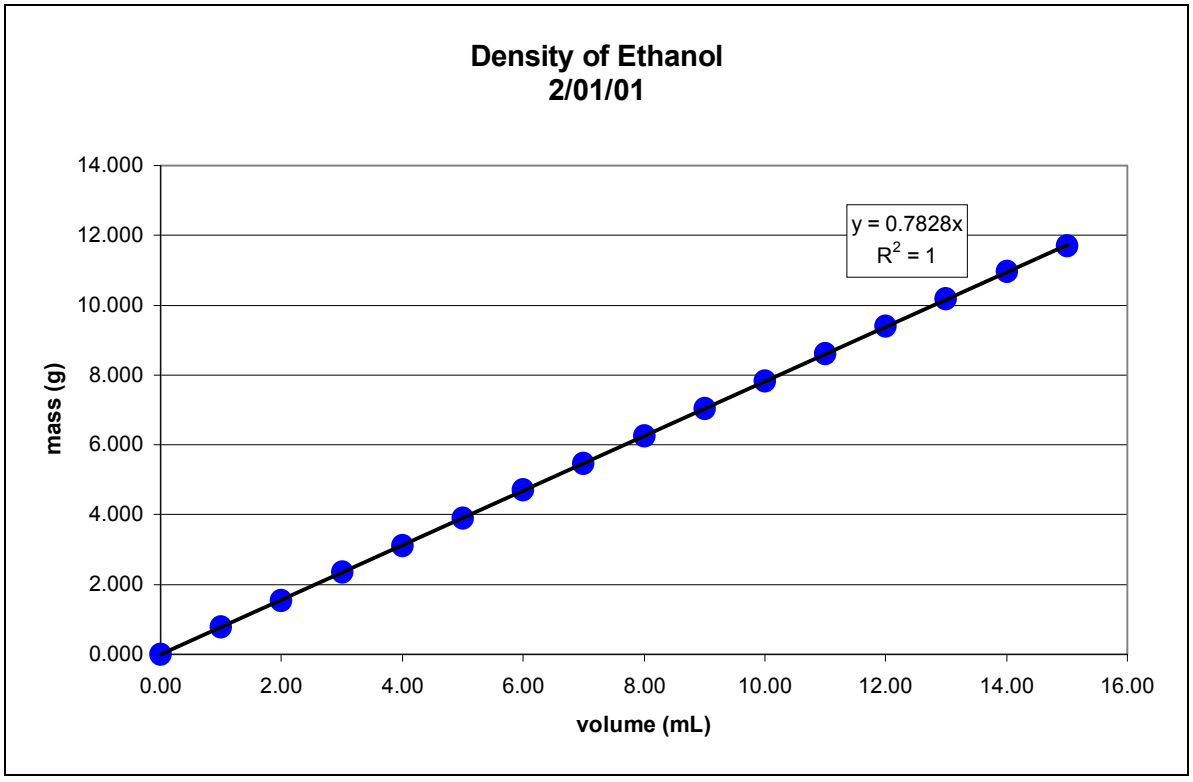

Figure 3: Density of Ethanol, 0.78 ± 0.01 g/mL

4.2.3. *Mouse & Rat Urine*

The urine used was provided by STAR Enterprise. Batch numbers were given to each sample according to the date it was received. Collection information is provided in Appendix A. The density of each batch of urine was recorded as soon as possible after the batch was received. Figures 4-10 show mouse urine density, while figures 11-13 show rat urine density. Only figure 4 was generated using the analog pipette method, all other figures' data was collected using the digital pipette method. Note that the density of male rat urine is consistently less than 1.00 ± 0.01g/mL. All data was collected at 23.3°C, 1.00 atm, and 23% relative humidity.

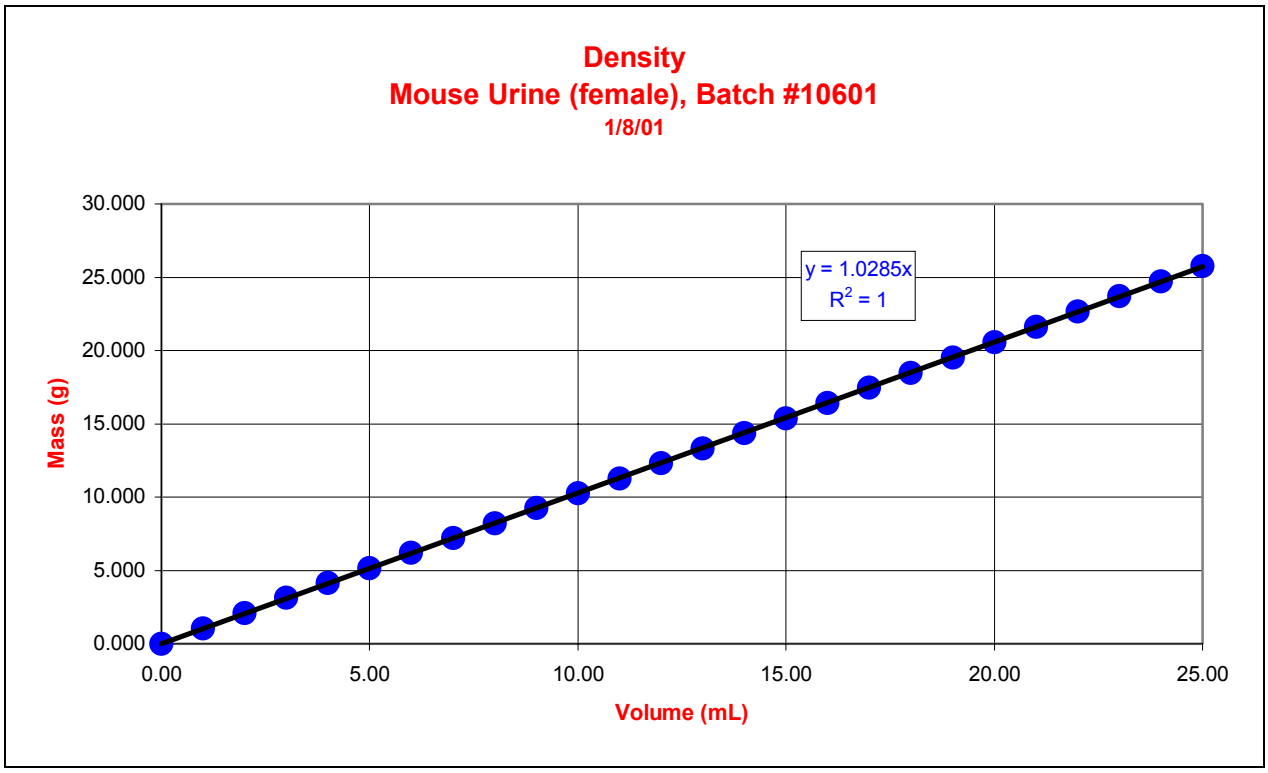

Figure 4: Density of mouse urine is 1.03 ± 0.05g/mL, batch#10601.

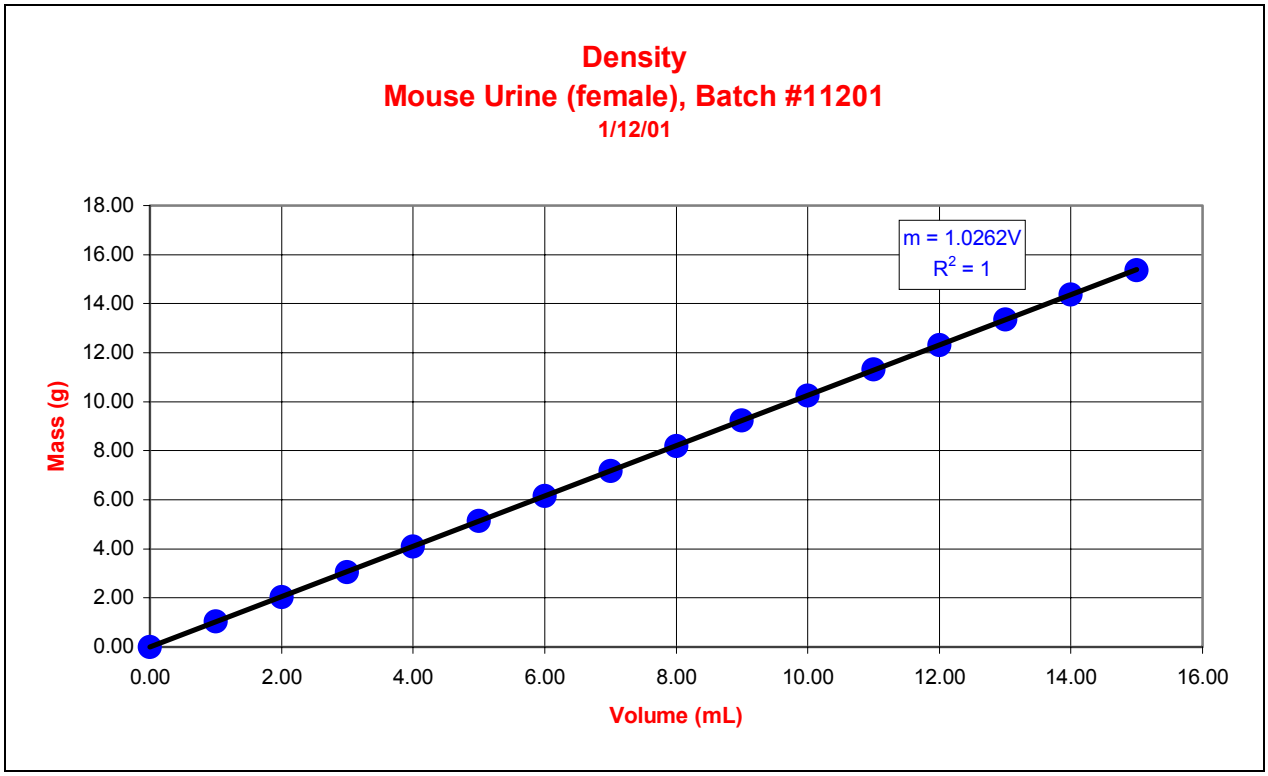

Figure 5: **Density of female mouse urine, batch #11201, according to the slope is 1.03 ± 0.01g/mL.**

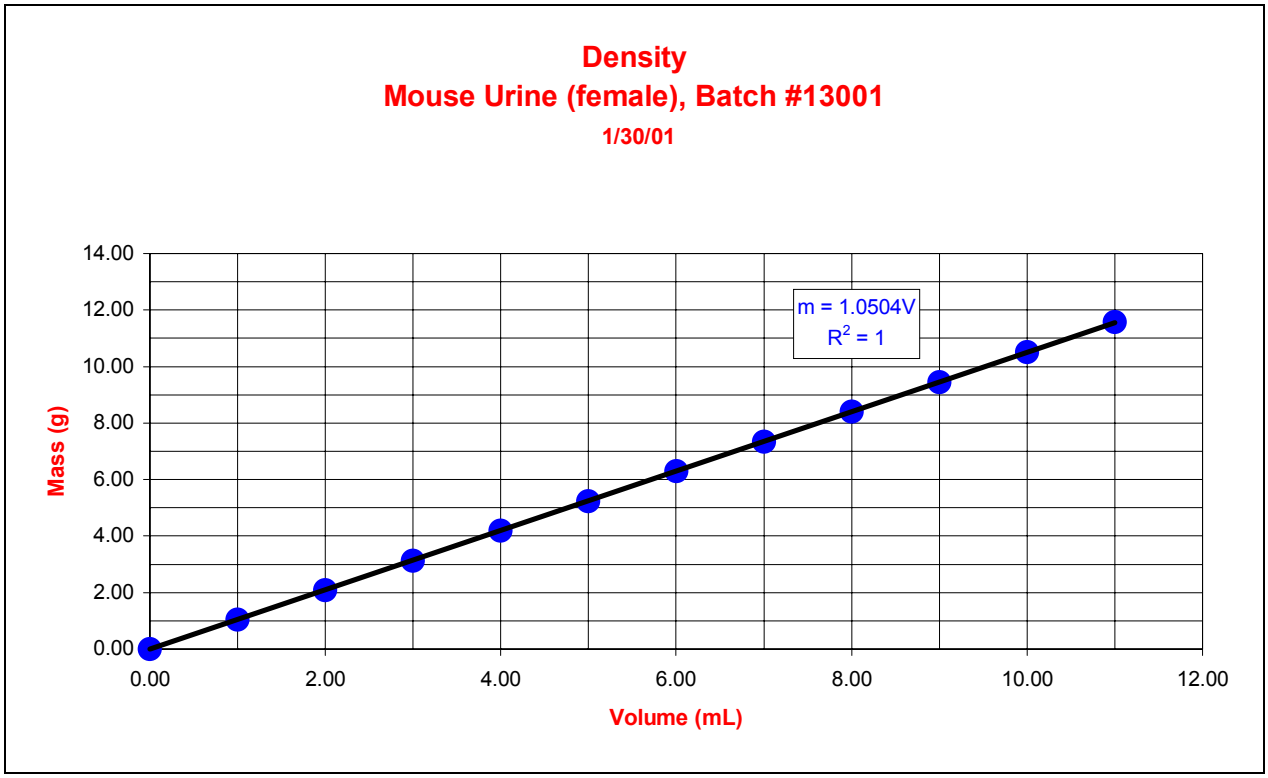

Figure 6: **Density of mouse urine batch #13001 is 1.05 ± 0.01g/mL.**

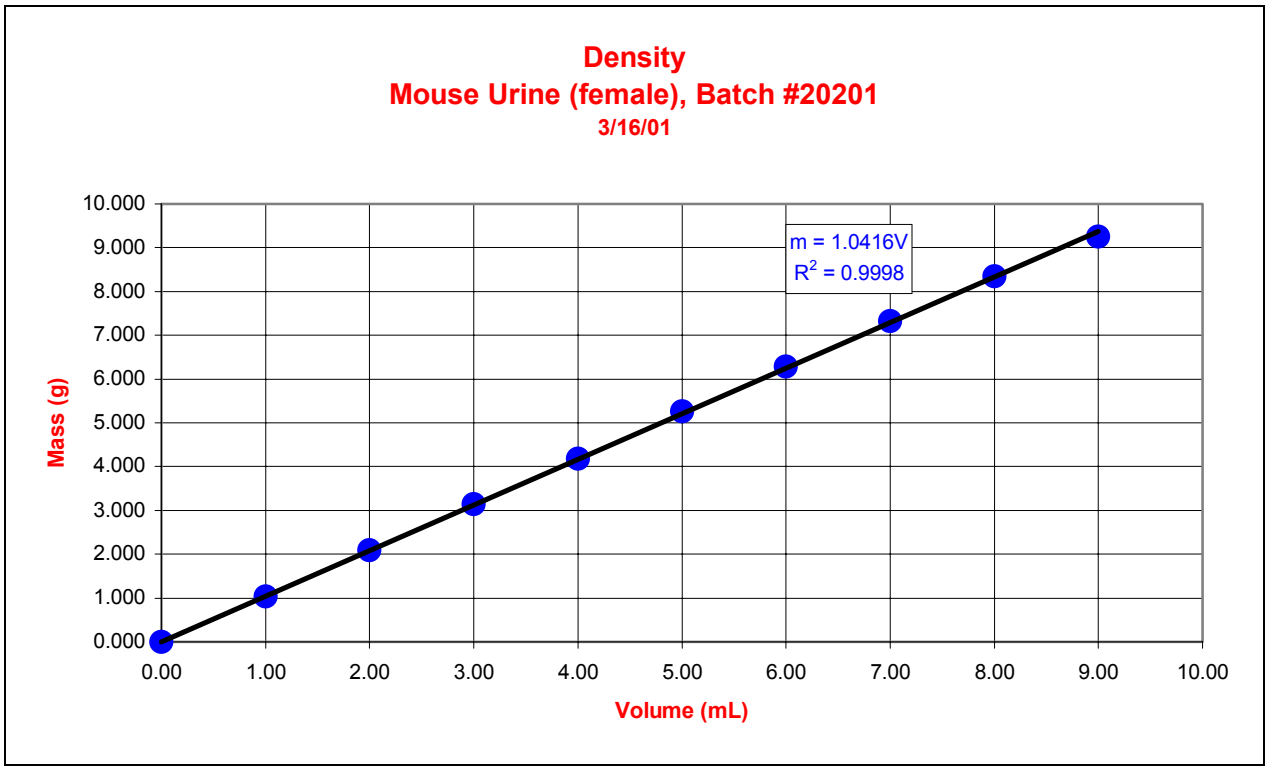

Figure 7: **Density of batch #20201 is 1.04± 0.01g/mL**

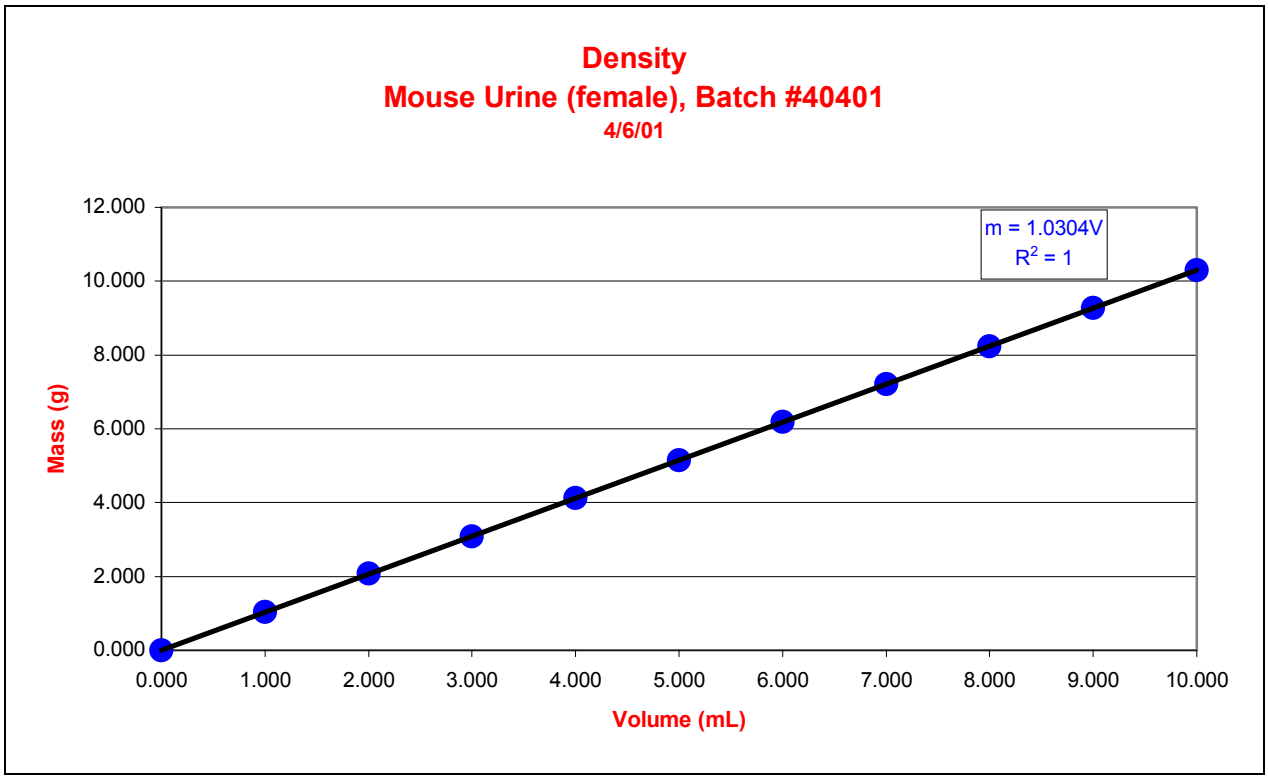

Figure 8: **Density of female mouse batch #40401 is 1.03± 0.01g/mL**

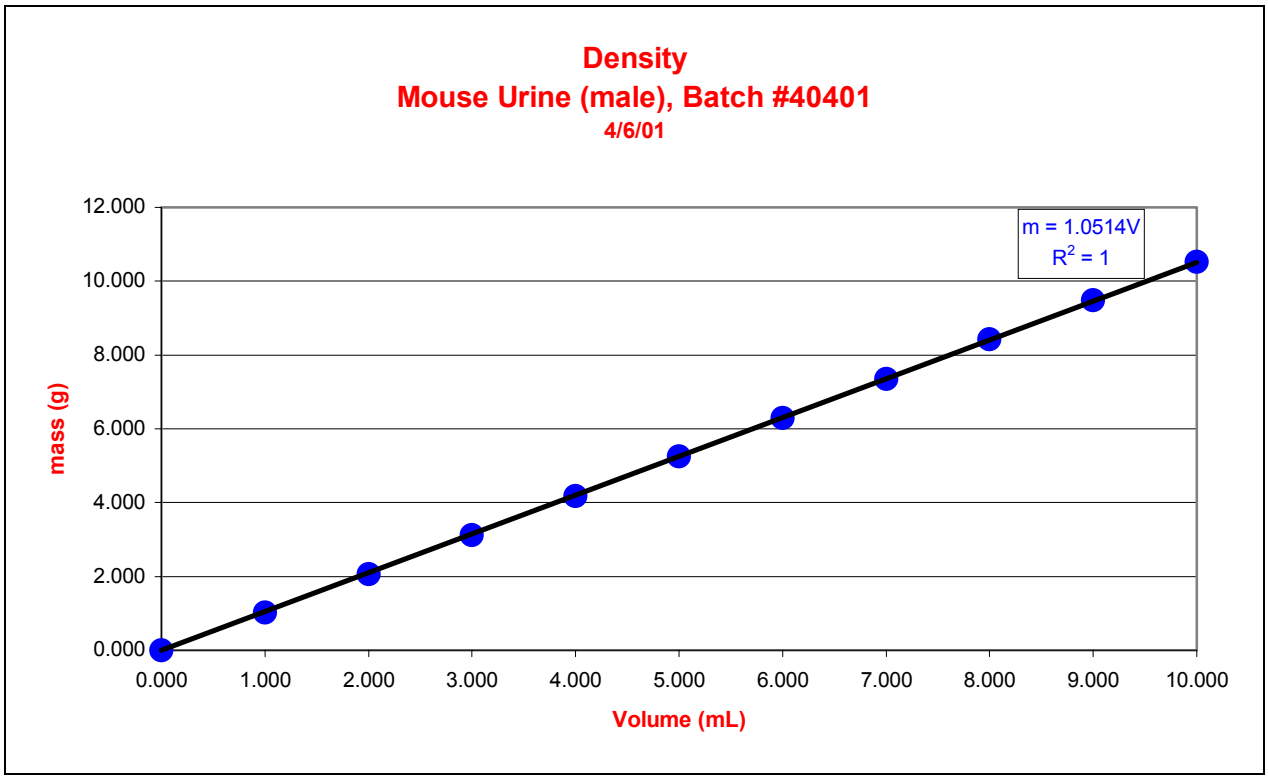

Figure 9: **Density of male mouse batch #40401 is 1.05 ± 0.01g/mL.**

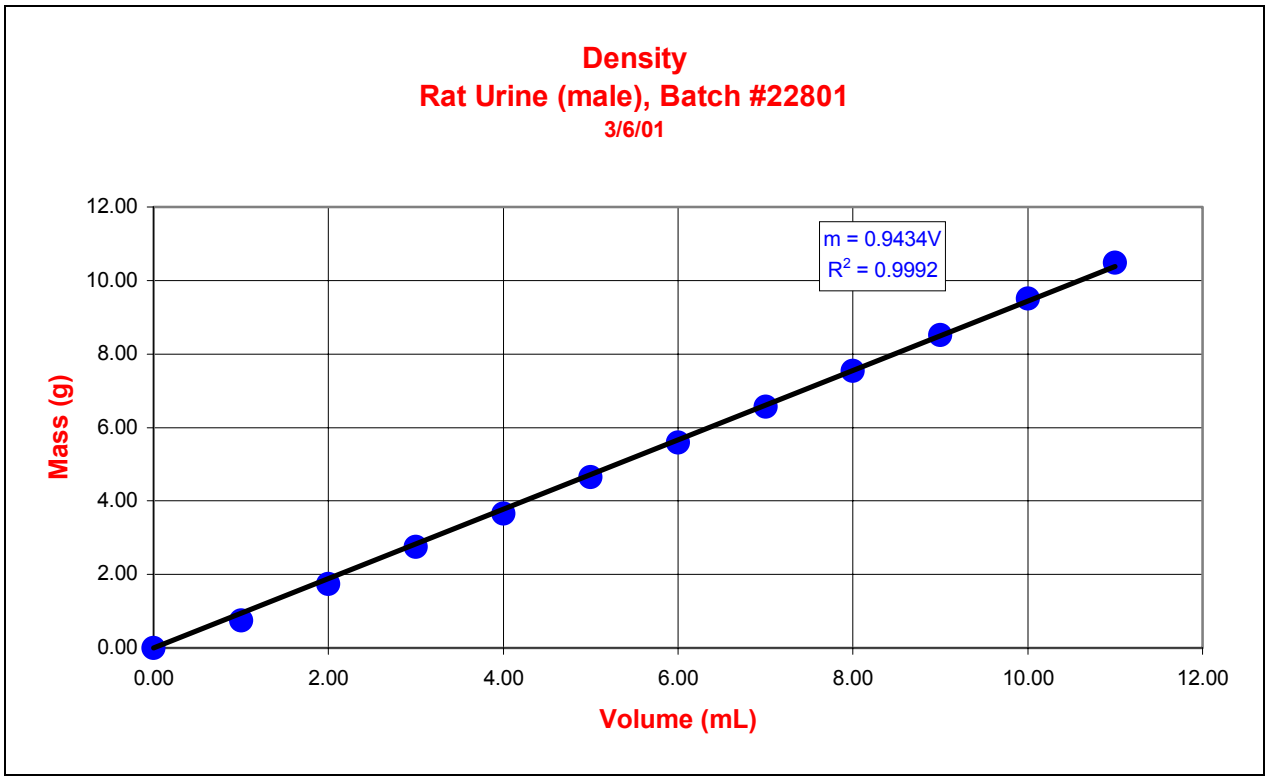

Figure 10: **Density of male rat urine batch #22801 is 0.943 ± 0.01g/mL.**

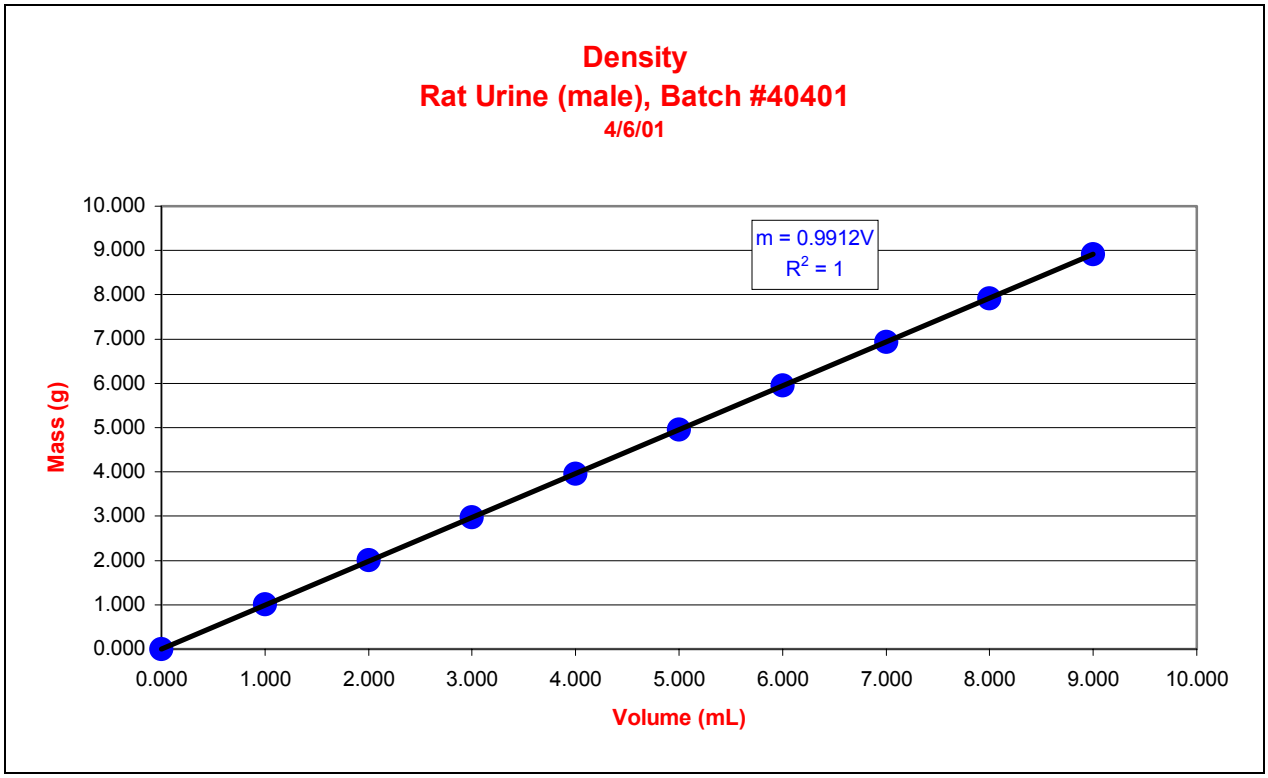

Figure 11: **Density of male rat urine batch #40401 is 0.99 ± 0.01g/mL.**

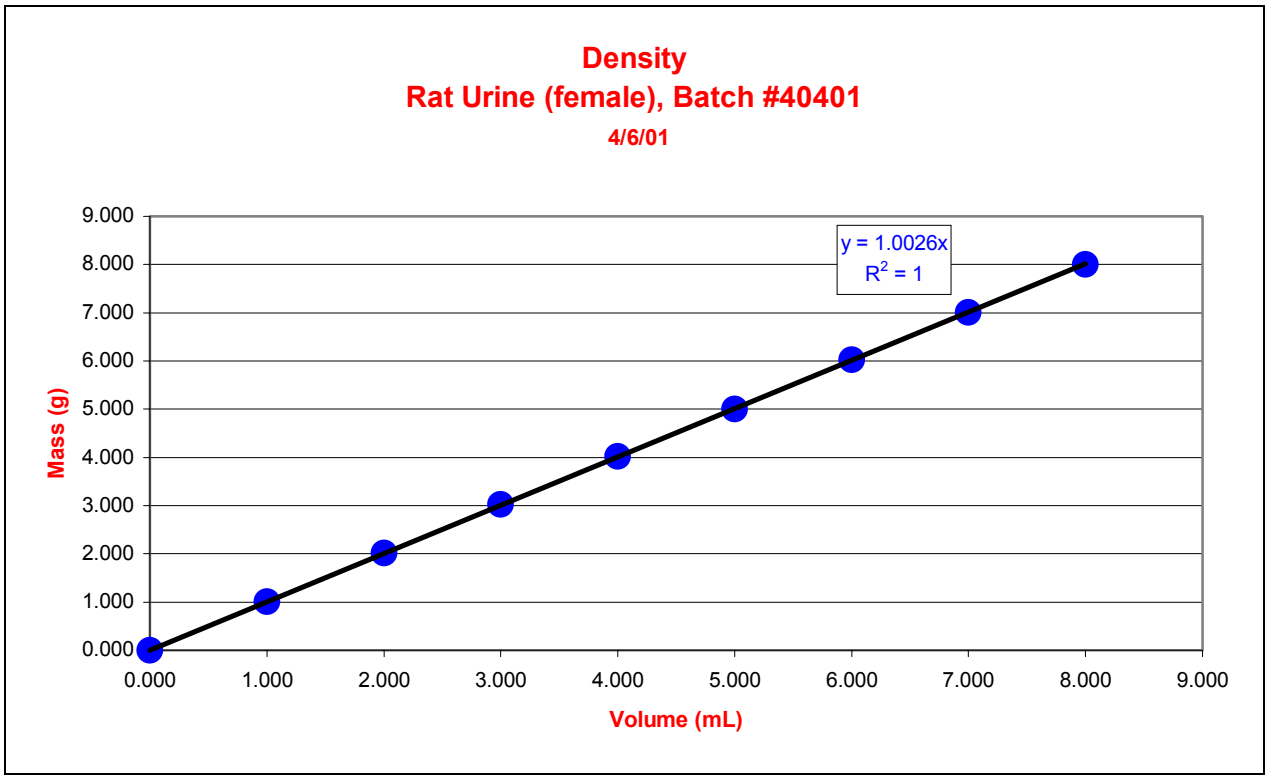

Figure 12: **Density of female rat urine batch #40401 is 1.00 ± 0.01g/mL.**

4.3. Analysis

Male and female mouse urines were similar in density with an average of 1.04 ± 0.01g/mL. Rat urine was less dense than mouse urine. Male rat urine had a density slightly less that water, averaging 0.98 ± 0.01g/mL. Female mouse urine was measured to be approximately 1.00±0.01g/mL. Error was calculated according to the ASME International standard for reporting experimental error.[2]

5. VISCOSITY

5.1. Methods and Materials

Calibrated Cannon-Fenske routine-type and reverse-flow tubes (sizes 50-150) were used to determine the efflux time of each fluid (see figure 13). The size of the tube was selected by approximating the viscosity (e.g. relative to water) of the fluid to be analyzed. The tube must be small enough so the efflux time between lines of descent (or ascent, with reverse-flow type) could be measured with a stopwatch. For example, a liquid with very low viscosity will move through a large tube too quickly to be measured macroscopically.

Measurements were taken using the ASTM standard D 446[3] and D 2170[4]. The tubes were charged with a volume specified by the calibration certificate supplied by the manufacturer. A digital Labsystems Finnpipette® (1-5mL) pipette was used to measure the volume of liquid. The liquid was dispensed into the larger of the two openings in the u-tube. The viscometer tube was positioned into a universal holder and the unit was placed into a Cannon CT-1000 constant temperature bath (figure 13). The bath was adjusted to the selected temperature and the liquid was allowed to equilibrate to this temperature (approximately 15 minutes). To avoid evaporation of the liquid between measurements, Parafilm® was placed over the two openings in the tube.

When the liquid reached the selected temperature, a pipette bulb was attached to the small opening and the liquid was suctioned just past the "starting line". A stopwatch was used to measure the time, in seconds, taken for the liquid to move from the start to finish line. In the reverse-flow viscometer tube, two efflux times can be taken. At least three readings were taken per temperature to arrive at an average. The kinetic viscosity was determined by multiplying the efflux time by the constant provided by the manufacturer on the calibration certificate. Constants are specific to each manufactured tube.

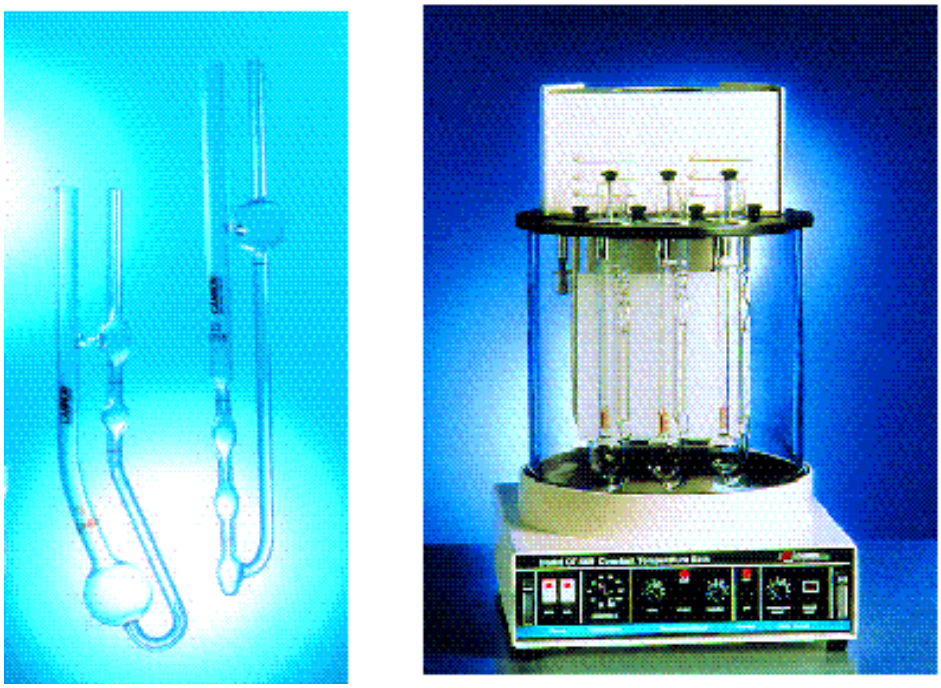

Figure 13: Constant temperature bath (left) and routine and reverse-flow viscometer tubes (right)

5.2. Results

5.2.1. *Viscometer Constant*

Coefficients given for each viscometer are specific to the given charge volume. With increasing charge volume, the constant decreases approximately according to the equation,

$$C = 0.0045V^{-0.1097} \qquad (5\text{-}1)$$

where C is the constant and V is the charge volume (figure 14). This graph shows that the constants are volume specific, and it is necessary to use the proper constant in order to determine accurate viscosity measurement.

If the filling temperature T_F was substantially different than room temperature, the viscometer constant was calculated at test temperature T_T, given by the equation

$$\text{Constant} = C_o[1+B(T_T + T_F)] \qquad (5\text{-}2)$$

The variables C_o and B are based on a coefficient of thermal expansion typical to that of mineral oil and are provided on the certificate of Calibration.

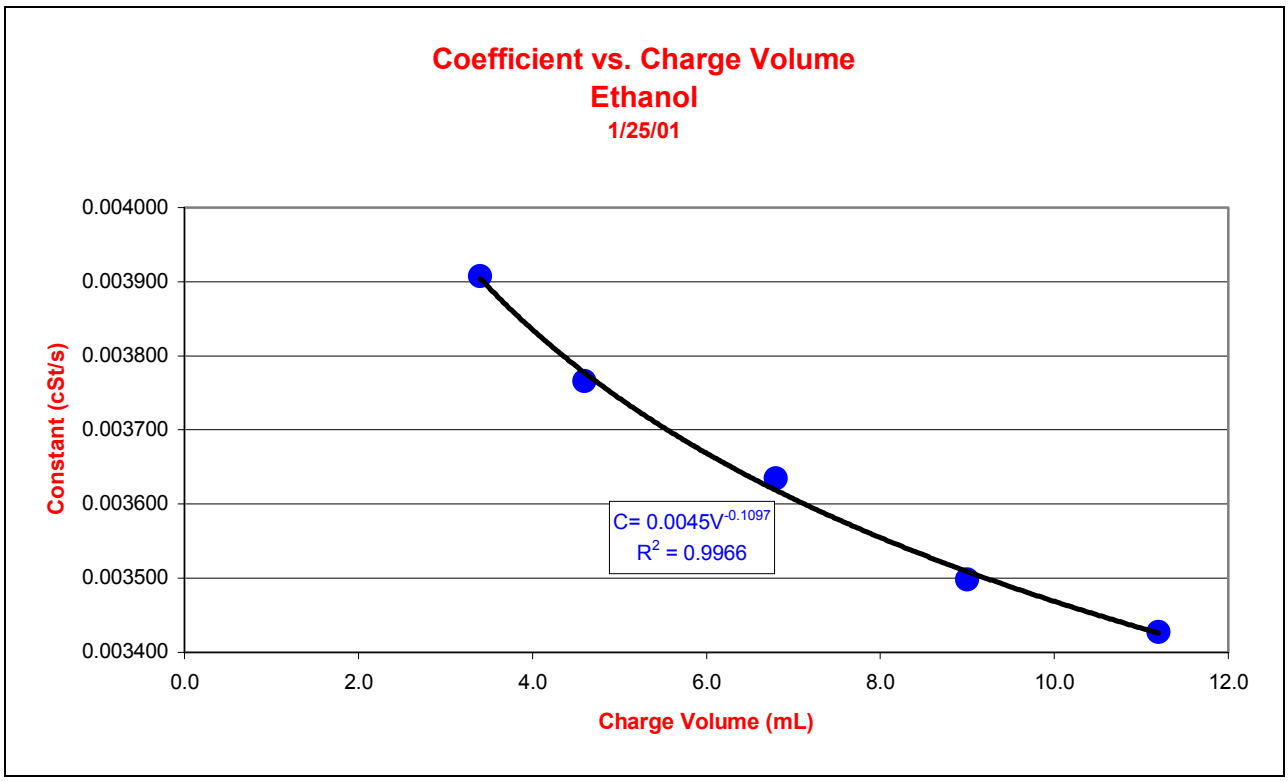

Figure 14: Variation of charge volume with charge volume. Routine-type tube used.

5.2.2. *Water and Urea*

To determine reproducibility of both procedures mentioned above, the viscosity of D.I.U.F. water at 23°C was recorded several times using a routine-type viscometer (size 50). The graph of the viscosity of water versus experimental trial number is shown in figure 15.

Urea was thought to be the main component of urine; therefore, the effect of mass fraction on viscosity was sought. The kinematic viscosity of an aqueous urea solution was measured with increasing mass fraction of urea. Routine (size 50) and reverse-flow (size 150) type viscometer tubes were used and the data was compared (see figure 16). The kinematic viscosity of a 20% urea solution was measured with increasing temperature. The viscosity of this solution decreases approximately according to the equation:

$$\upsilon = -0.0091\theta + 1.2306 \qquad (5\text{-}3)$$

where υ is the kinematic viscosity and θ is the temperature.

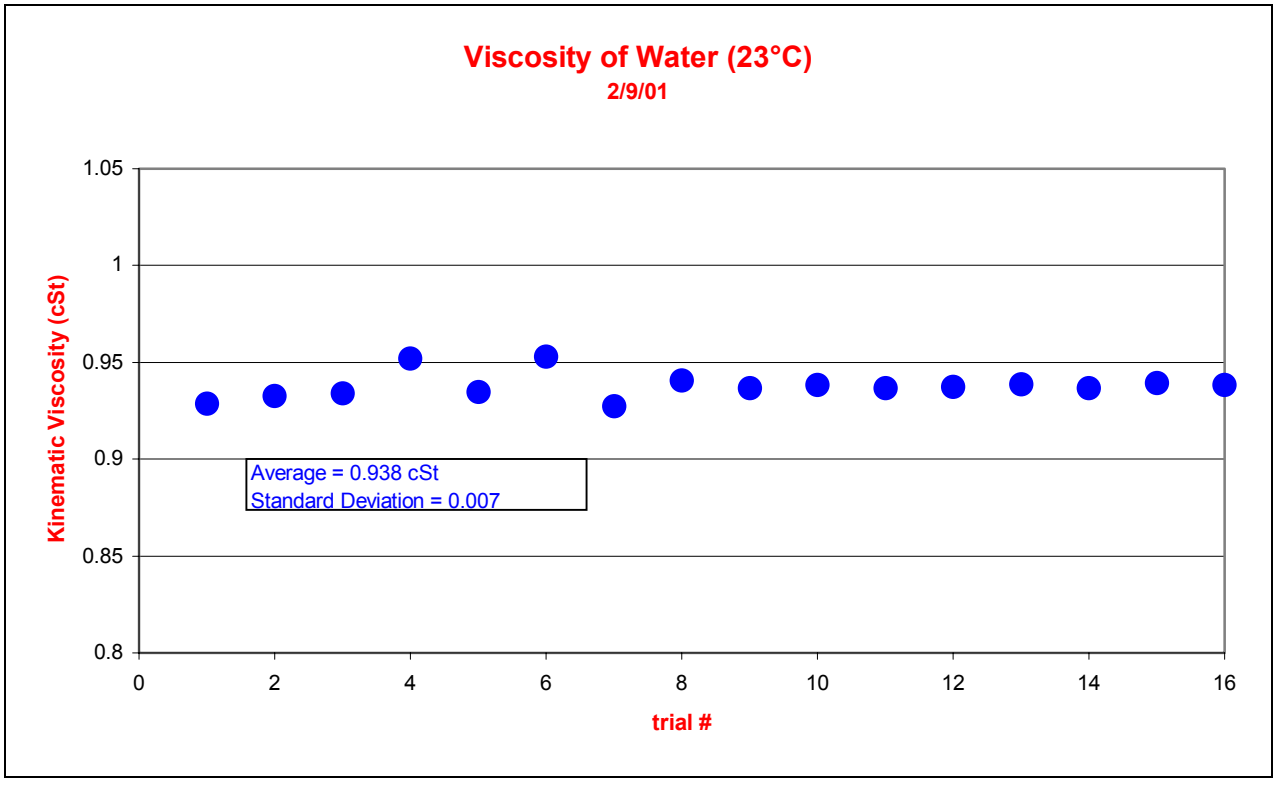

Figure 15: Kinematic viscosity of D.I.U.F water at 23°C was 0.94 ±0.07 cSt. Routine-type tube used.

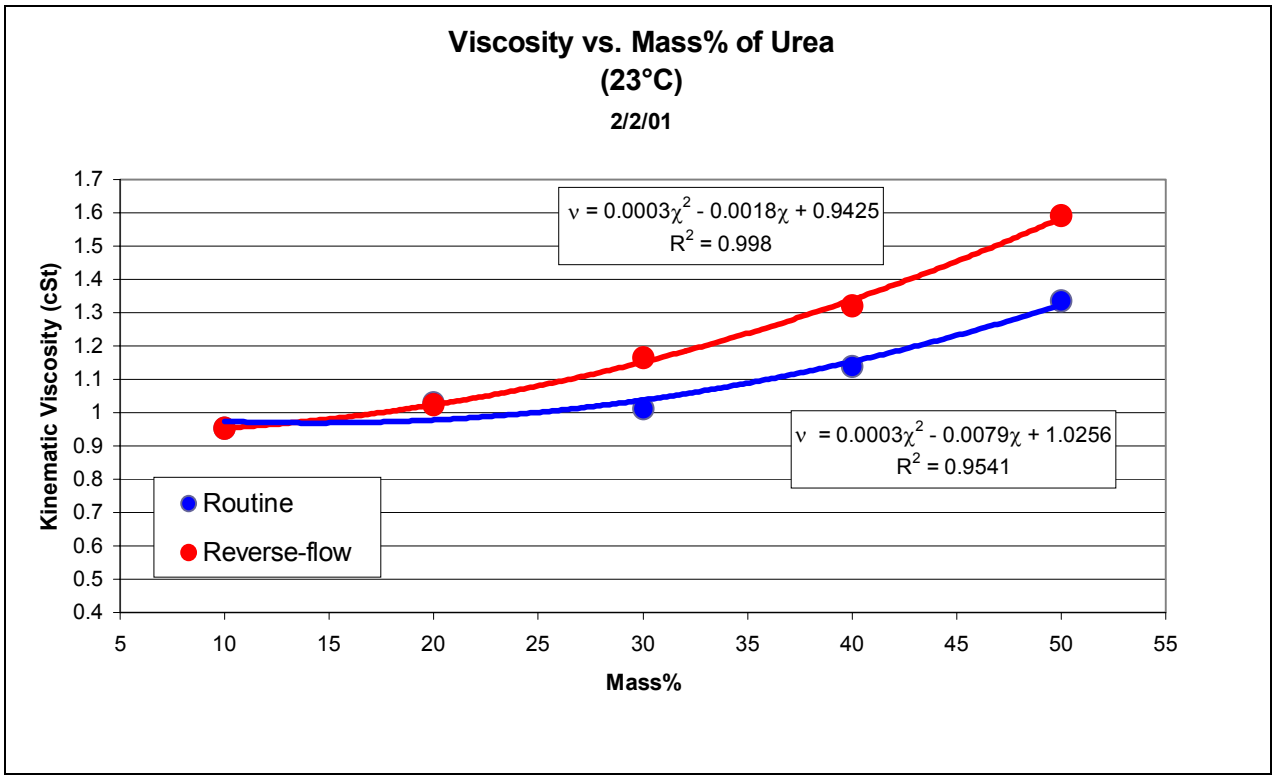

<u>Figure 16:</u> Kinematic viscosity of aqueous urea solution versus mass % of urea. The data was acquired using ASTM D446 for the routine type tube (blue) and ASTM D2170 for the reverse-flow type tube (red).

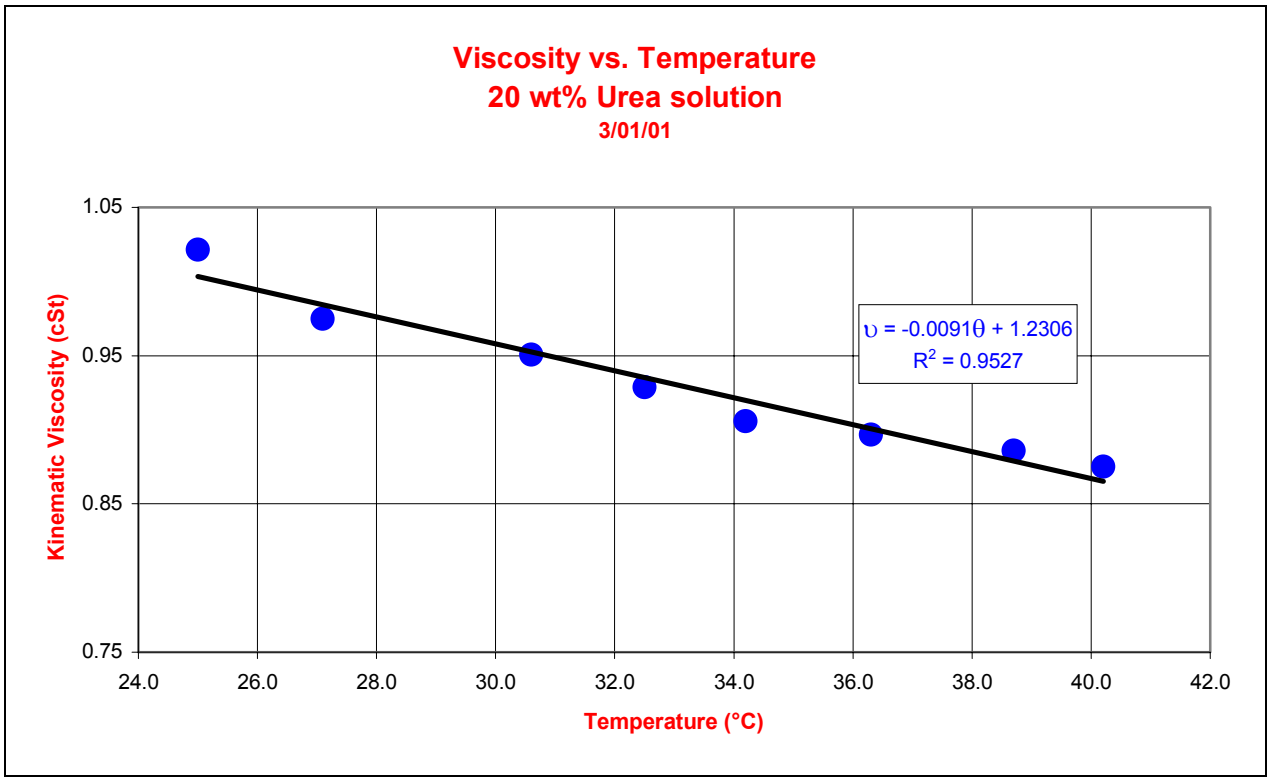

Figure 17: **Kinematic viscosity of 20% urea solution with temperature. Reverse-flow tube used (ASTM D2170).**

5.2.3. *Rat and Mouse Urine.*

The kinematic viscosity of mouse urine (batch #11201) at 23°C was recorded several times (see figure 18). The average kinematic viscosity was 1.122 cSt. The viscosities of mouse (batch #20201) and rat (batch #22801) urine were measured with changing temperature (figures 19-20).

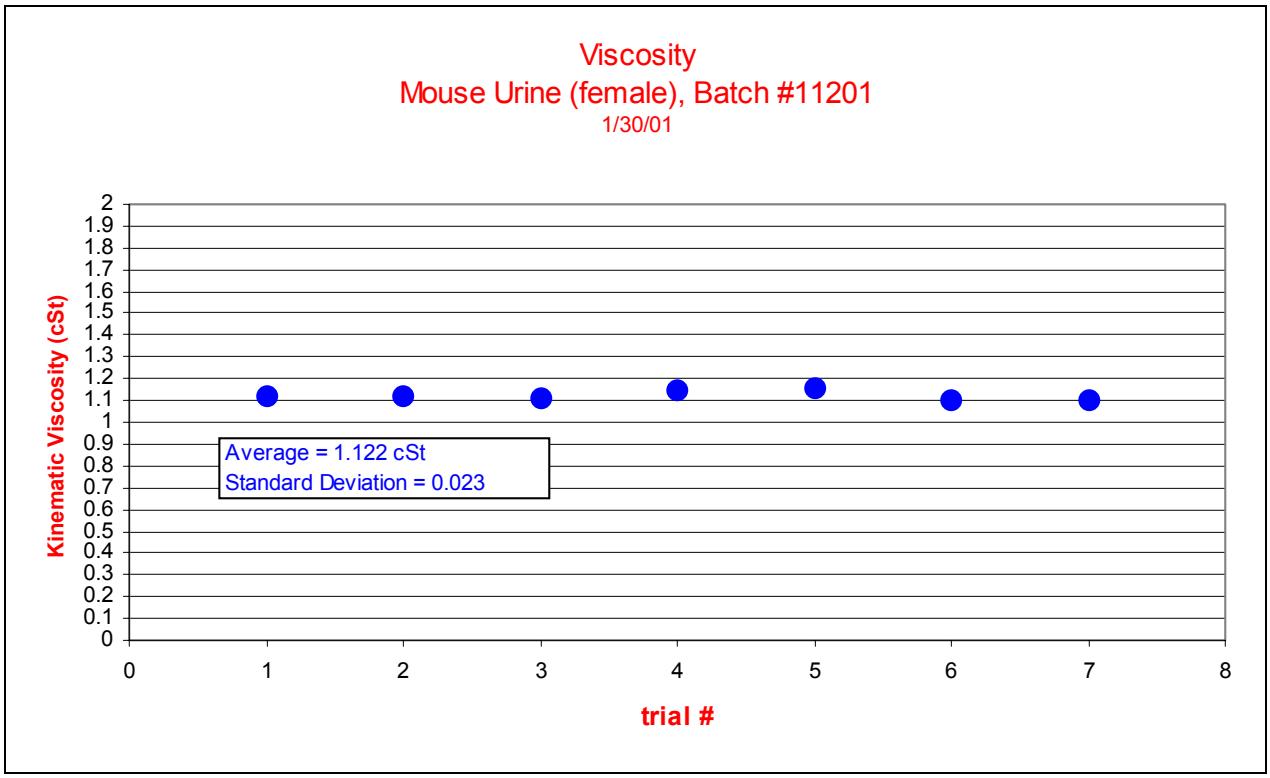

Figure 18: Kinematic viscosity of mouse urine at 23°C. average = 1.122cSt. Routine-type tube used.

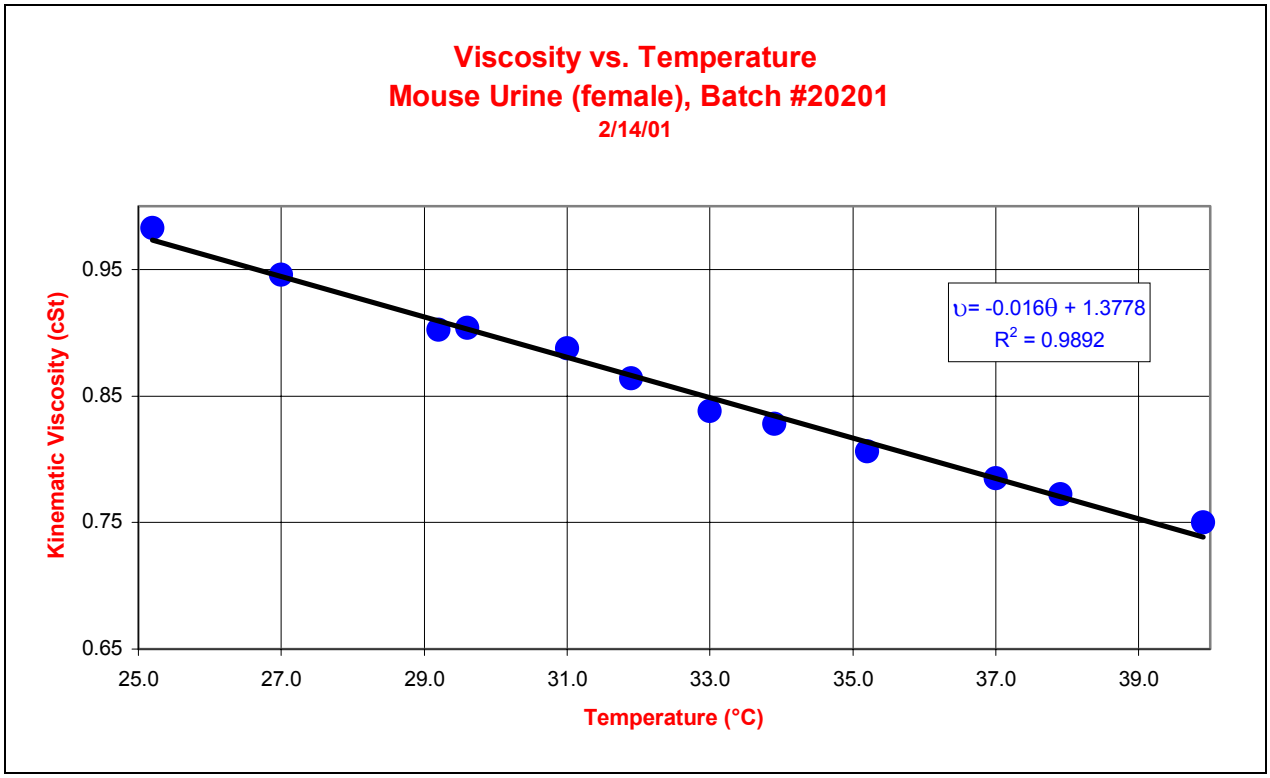

Figure 19: **Kinematic viscosity of female mouse urine decreasing with temperature. Reverse-flow tube used.**

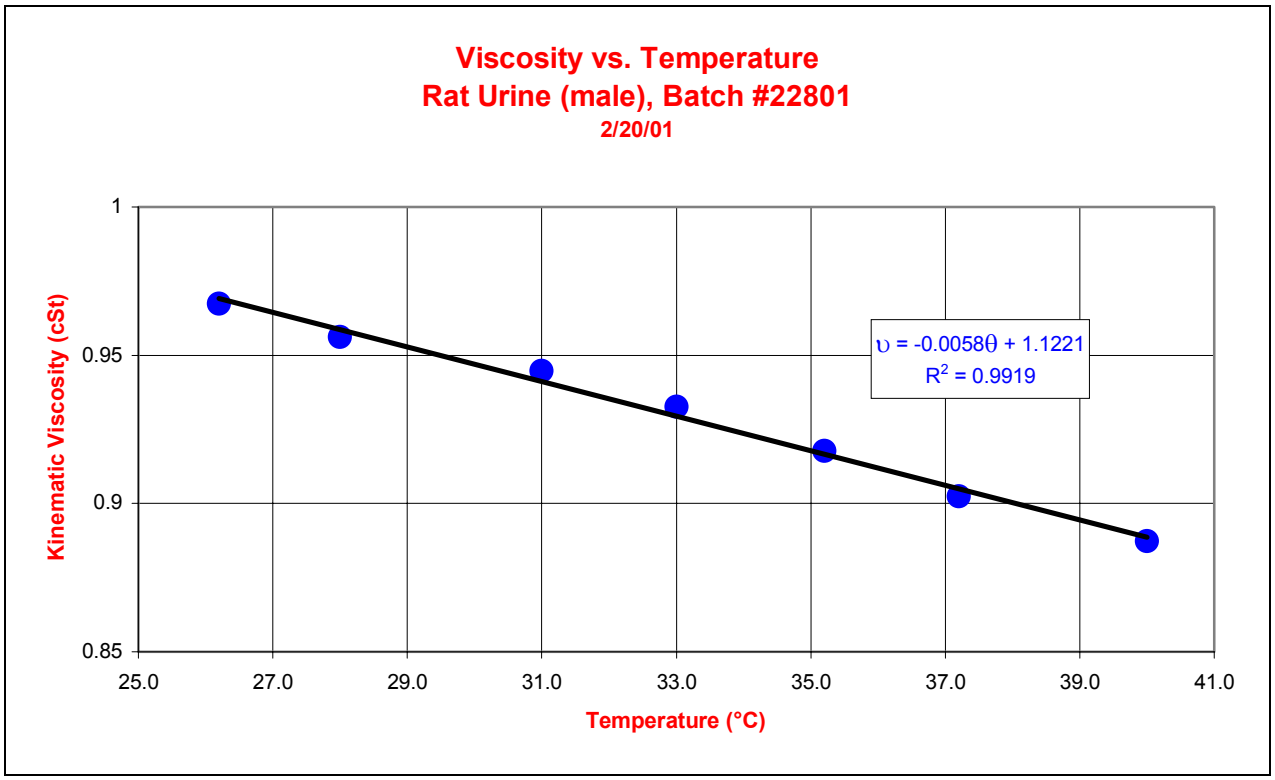

Figure 20: **Kinematic viscosity of male rat urine decreasing with temperature. Reverse-flow tube used.**

5.3. Analysis

A 20wt% aqueous urea solution was used because the density listed in the *CRC Handbook* was almost the same as mouse urine. The kinematic viscosity decreased as a function of temperature according to equation 5-3. For the batches tested, female mouse urine viscosity decreases at a slightly higher rate ($\nu=-0.016\theta+1.377$) while male rat urine decreases at a lesser rate ($\nu=-0.0058\theta+1.122$). Viscosity versus temperature data is important to understand how the viscosity of the urine changes when it is cooled from body temperature to room temperature. The graphs show that the mouse urine is less viscous than rat urine at body temperature until it reaches room temperature, where the viscosities are comparable.

The kinematic viscosity of an aqueous urea solution was tested versus mass percent of urea.. Both reverse-flow and routine tubes were used in this case. Aside from similar kinematic viscosity readings of the 10% urea solution, viscosity measurements of each tube differ, according to figure 16. It is possible the accuracy of the reverse-type tube is due to the fact that each data point is an average of two readings instead of one as in the case of the routine-type. At 50% urea, just before the solution achieves super-saturation, kinematic viscosity measurements differ by 0.25 cSt. When compared to data recorded for urea in the *CRC Handbook*, routine-type data differed by as much as 15% while reverse-flow data consistently differed by 1.3%. For this reason, all graphs of data subsequent to February 9, 2001 were produced using measurements acquired using reverse-flow tubes.

The primary source of human error arose during measurement of efflux times, resulting in an error of ±0.5 seconds or ±0.07 cSt. The expanded uncertainty with 95% confidence of the calibration measurement relative to the primary standard is ±0.34%.[c]

[c] *Certificate of Calibration.* Cannon Instrument Company. ©2000.

6. SURFACE TENSION

6.1. Materials and Methods

All liquids were investigated with a CAHN Dynamic Contact Analyzer 315 using the Wilhelmy plate method. The DCA 315 measures surface tension according to ASTM standard 971[5]. Surface tension is measured using the equation,

$$\sigma = (F - F_b)/(L*\cos\theta) \qquad (6\text{-}1)$$

where F and F_b are the measured force and buoyancy force correction, respectively, L is the perimeter of the immersing edge of the plate, and θ is the contact angle. A treated platinum plate is used with which the contact angle is zero and the surface tension is directly proportional to the force.

The DCA 315 was calibrated according to the manufacturer's instructions. The liquid was placed into a small, fairly shallow container such as a Corning #430165 cell culture dish (35mm x 10mm). The dish was wide enough to avoid interaction with the immersing platinum plate. A clean, dry platinum plate was attached to the holder provided by the manufacturer and hung from the diamond hang-down loop. The container was placed on the DCA315 moveable stand directly underneath the plate.

WinDCA software was used in conjunction with the DCA315 for data acquisition. The DCA315 was programmed to perform a cycle, typically:

- Set speed (80-264μm/s)
- Detect zero depth of immersion (ZDOI)
- Advance
- Return to ZDOI
- Recede to maximum force
- Return to zero position

The software recorded the change in force in terms of weight versus change in position of the plate during the cycle. After converting the maximum receding mass into a force, the surface tension was acquired using equation 6-1. Between each test, the platinum plate was cleaned with a wash of distilled water and isopropanol. Each data point is an average of three measurements.

6.1.1. *Surface Tension vs. Temperature*

To detect the change in surface tension with temperature, a CAHN DCA series temperature control unit was used. This component was installed into the DCA315 and used in conjunction with a NESLAB RTE-110 to circulate a 50% ethylene glycol solution through the water jacket of the temperature control unit. This setup is shown in figure 21. The RTE-110 was set to the desired temperature and the sample was placed in the temperature control unit vessel. The sample was covered with Parafilm® and allowed to reach the desired temperature. The Parafilm® was then removed and the surface tension was acquired using the above method.

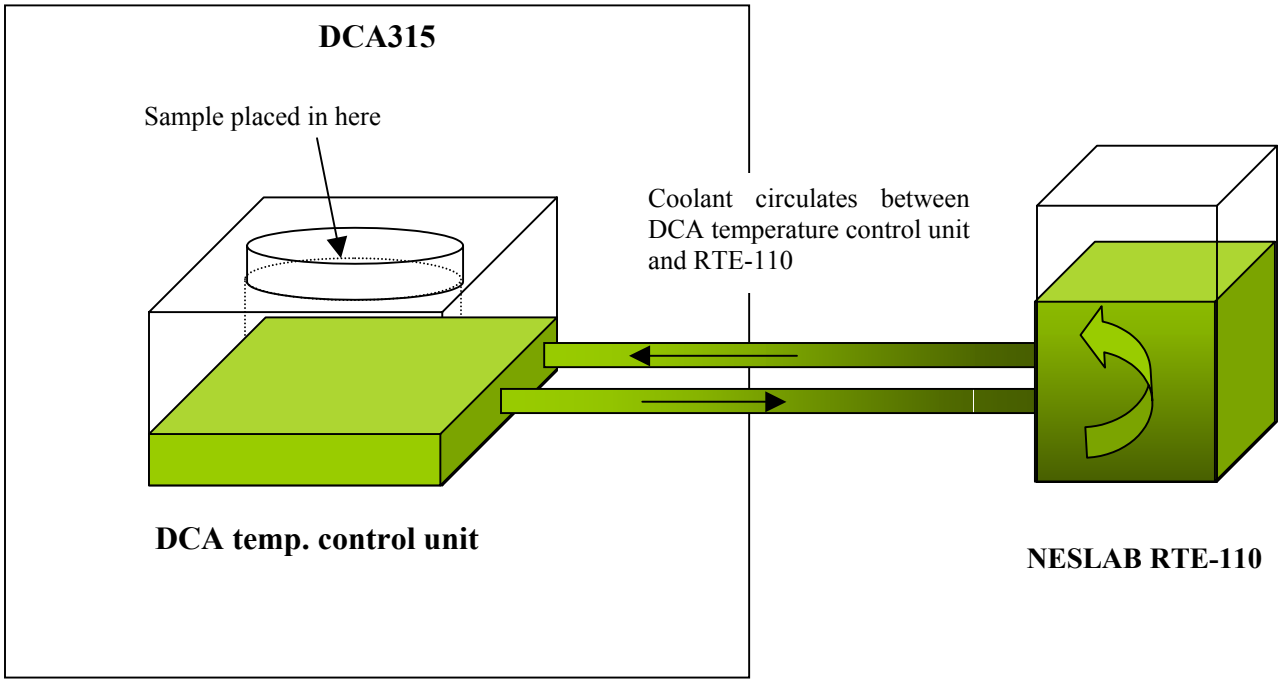

Figure 21: Temperature control setup.

6.2. Results

6.2.1. *Water and Aqueous Solutions*

To examine both the reproducibility of the above protocol and the accuracy of the WinDCA software, the surface tension of D.I.U.F. water was initially tested. Figure 22 shows the difference between manually calculated data and data calculated by the software. On average, the surface tension was 71.52 ± 0.5 mN/m.

Aqueous solutions of urea, sucrose, and sodium chloride were examined in attempts to find a surrogate solution for the rodent urine. The surface tensions of these aqueous solutions varying with mass percent of the solute can be seen in figures 24-25. Figure 24 shows that the surface tension of the sucrose solution does not change as more solute is added. Addition of salt to water increases the surface tension approximately with the equation,

$$\sigma = 0.1952\chi + 70.985 \qquad (6\text{–}2)$$

where χ is the mass percent of the solute. Addition of urea tends to decrease the surface tension approximately with the equation,

$$\sigma = -0.3276\chi + 71.966 \qquad (6\text{-}3)$$

as seen in figure 25.

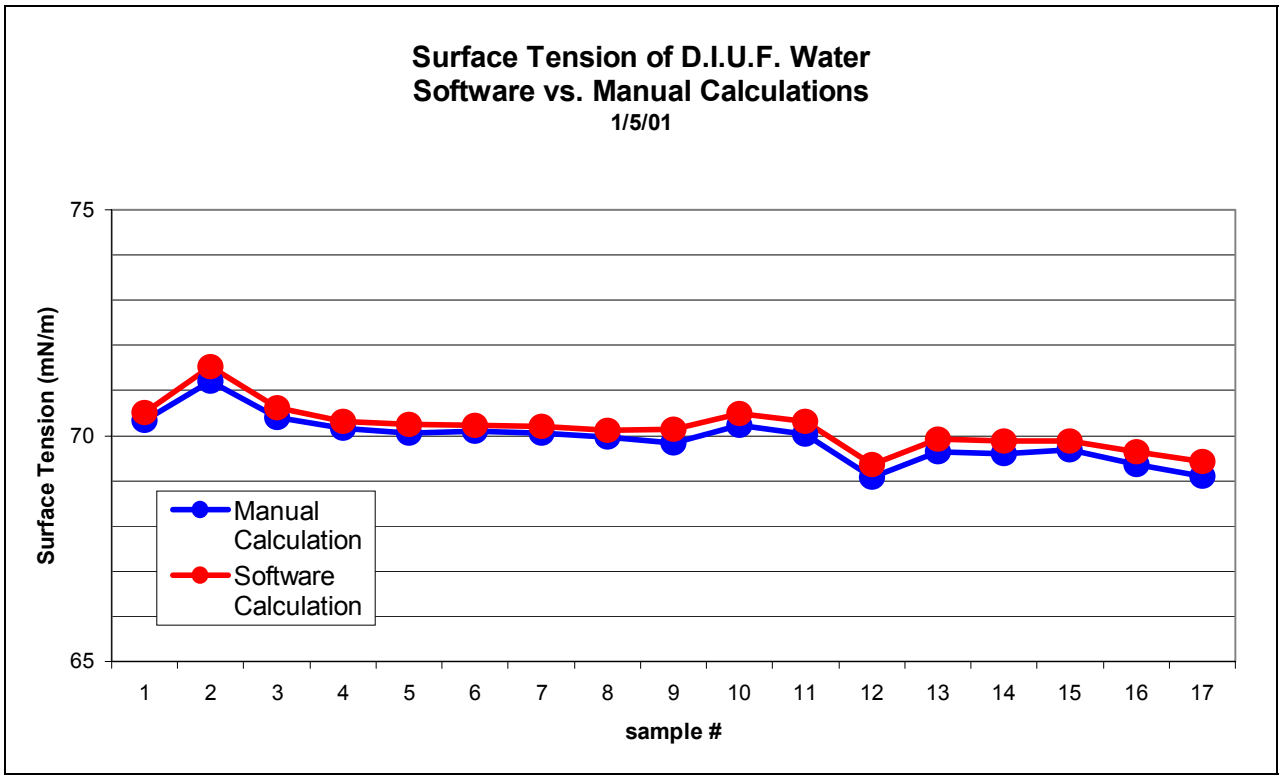

Figure 22: **Surface tension of D.I.U.F. water, manual vs. software calculations.**

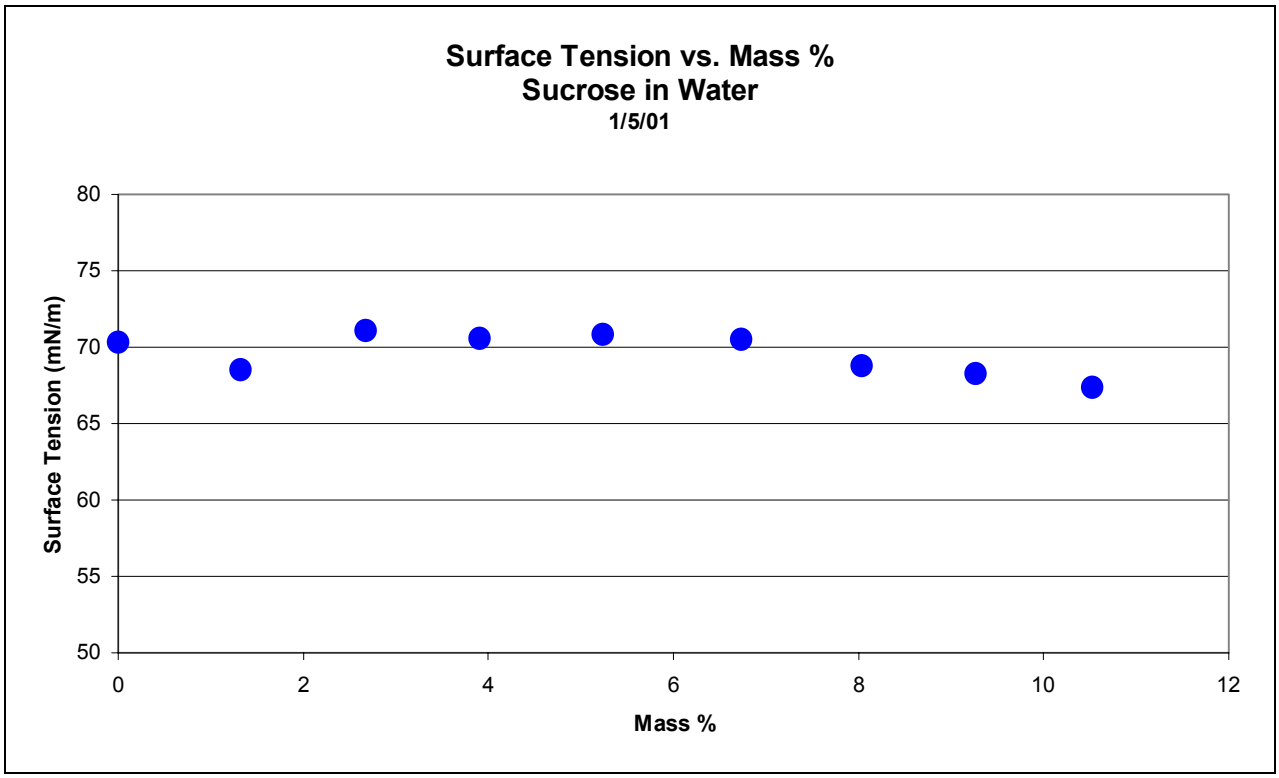

Figure 23: **Surface tension variation with increasing mass % of sucrose in water.**

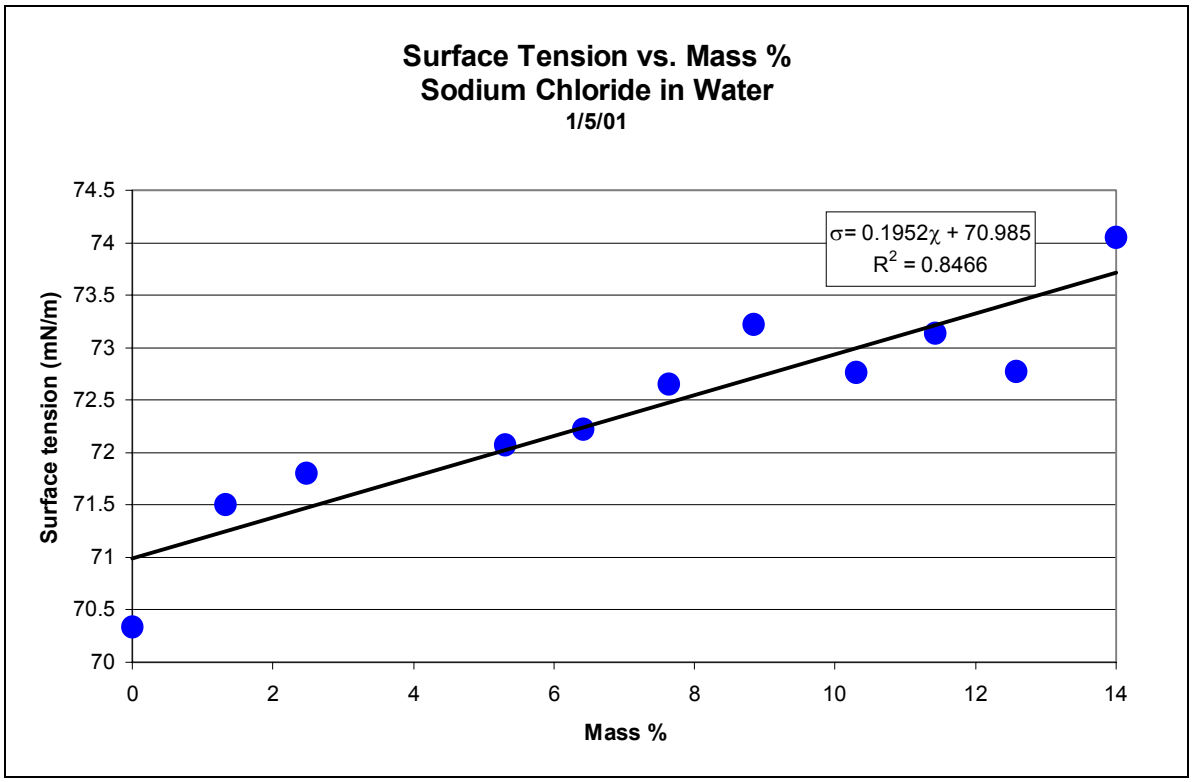

Figure 24: **Surface tension variation with increasing mass % of sodium chloride.**

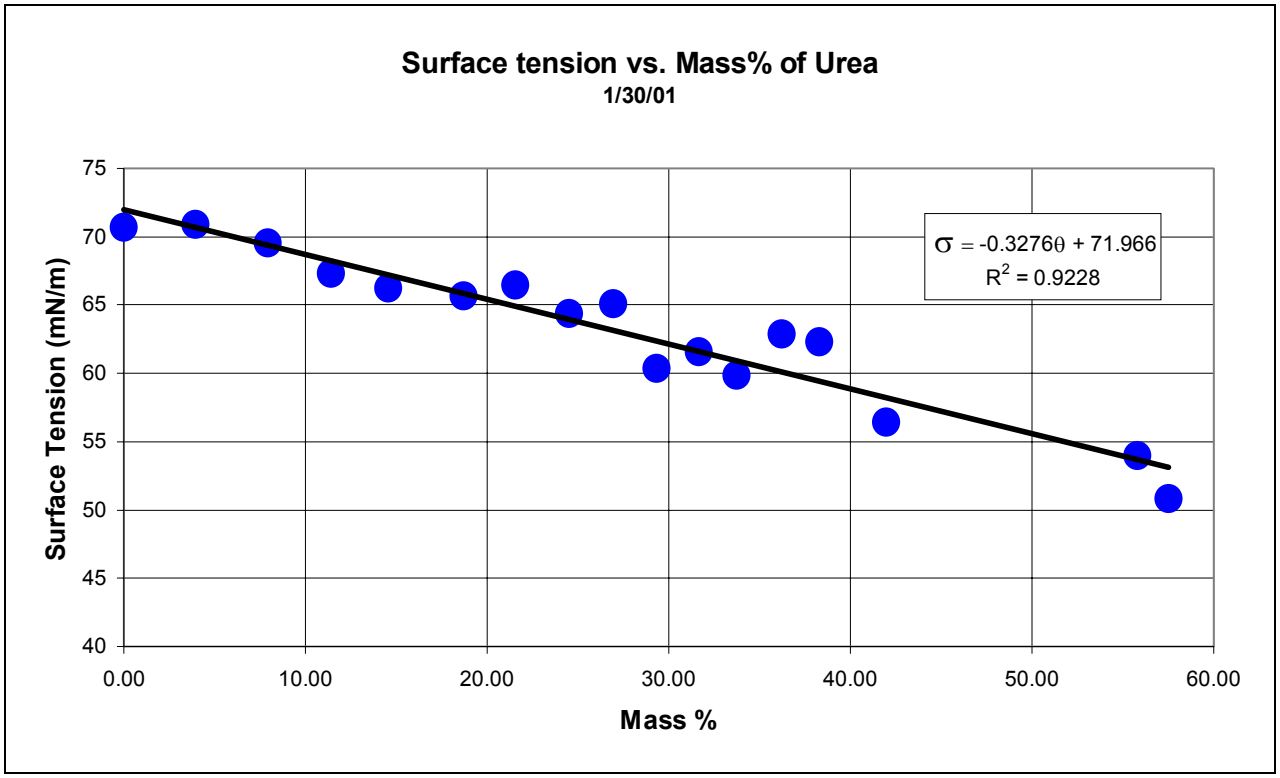

Figure 25: **Surface tension with increasing mass% of urea.**

6.2.2. *Rat and Mouse Urine*

On average, the surface tensions of unfiltered (batch #10601) and filtered (batch #13001) mouse urine at 23°C were 37.61 and 46.68 mN/m, respectively (figures 26-27). See section 3.1 for more details on the filtration methods. The surface tension of rat urine (batch #22801) at 23°C was 36.47 mN/m (figure 28)

Surface tension readings of the rat and mouse urine were also taken at various temperatures. Figure 29 shows that the surface tension of mouse urine changes very little with increasing temperature. Figure 30 shows that the surface tension of rat urine decreases with temperature according to the equation,

$$\sigma = -0.0003\theta^3 + 0.0203\theta^2 - 0.576\theta + 42.313 \qquad (6\text{–}4)$$

where θ is the temperature of the urine.

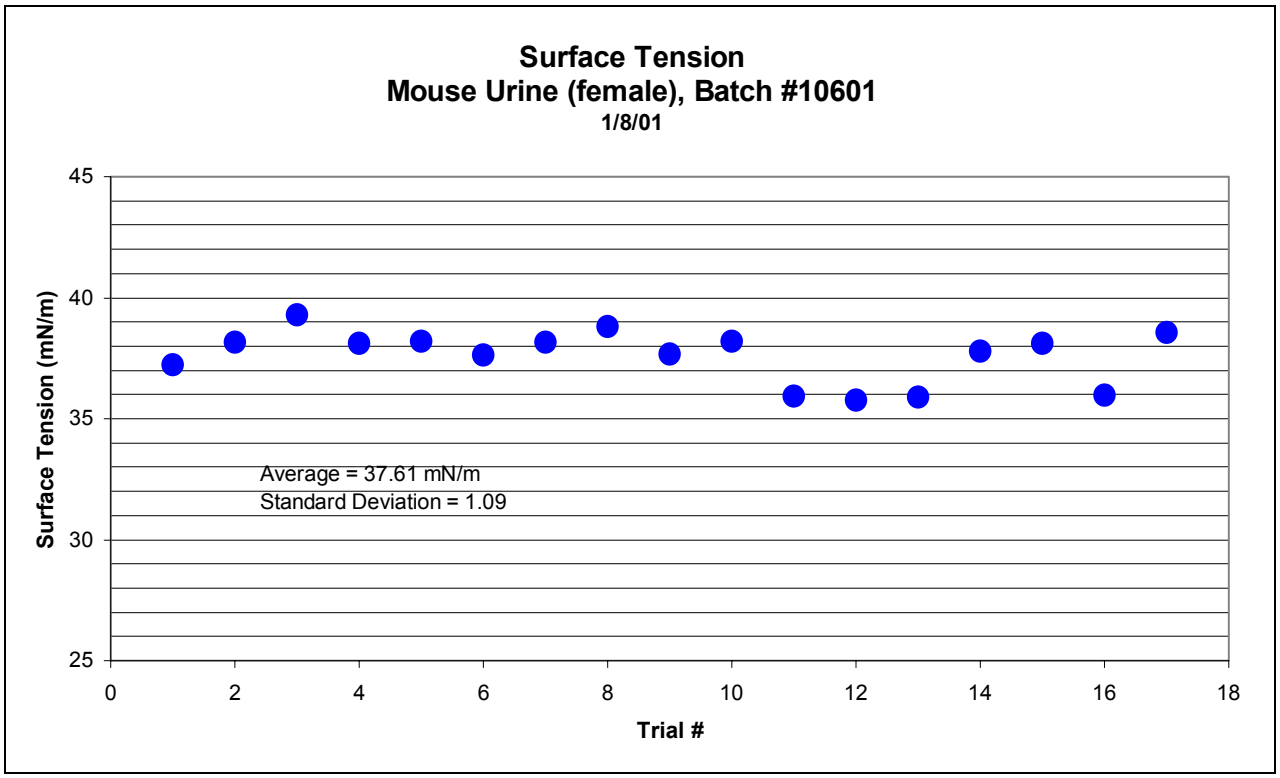

Figure 26: Surface tension of unfiltered mouse urine at 23°C.

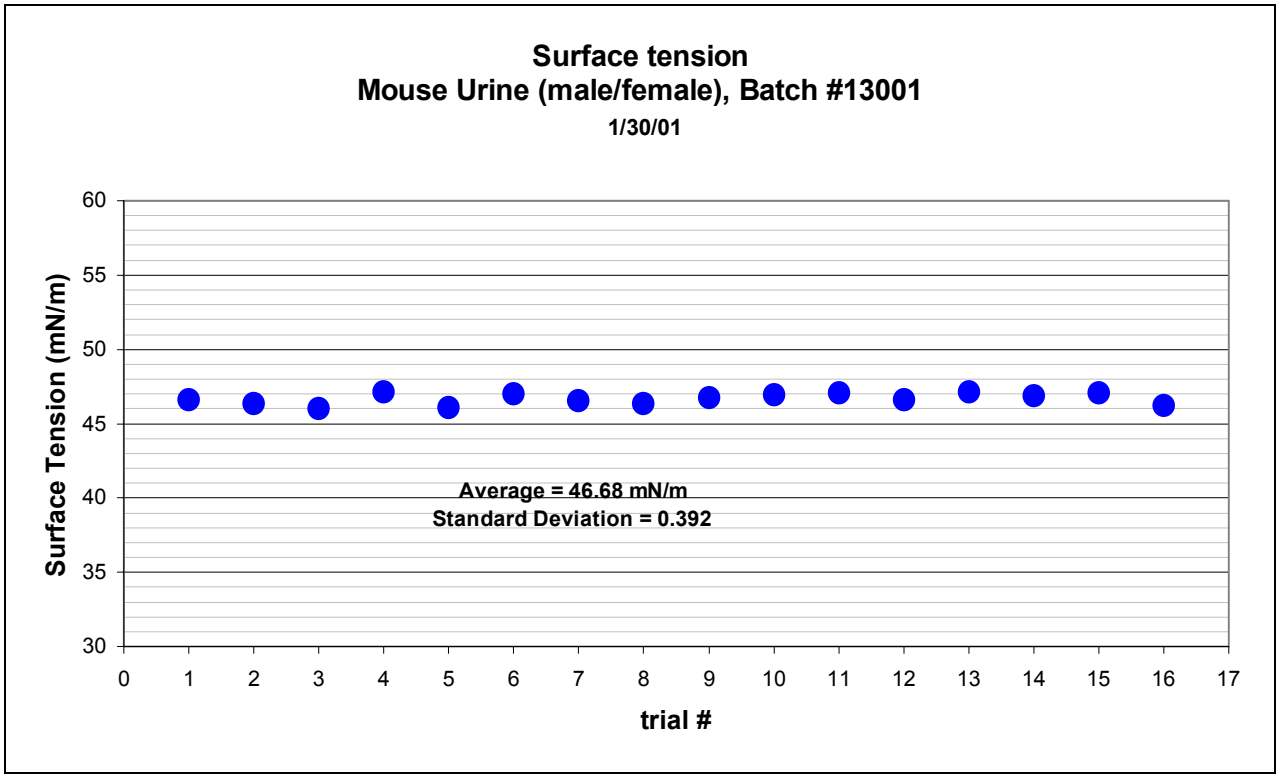

Figure 27: **Surface tension of filtered mouse urine at 23°C.**

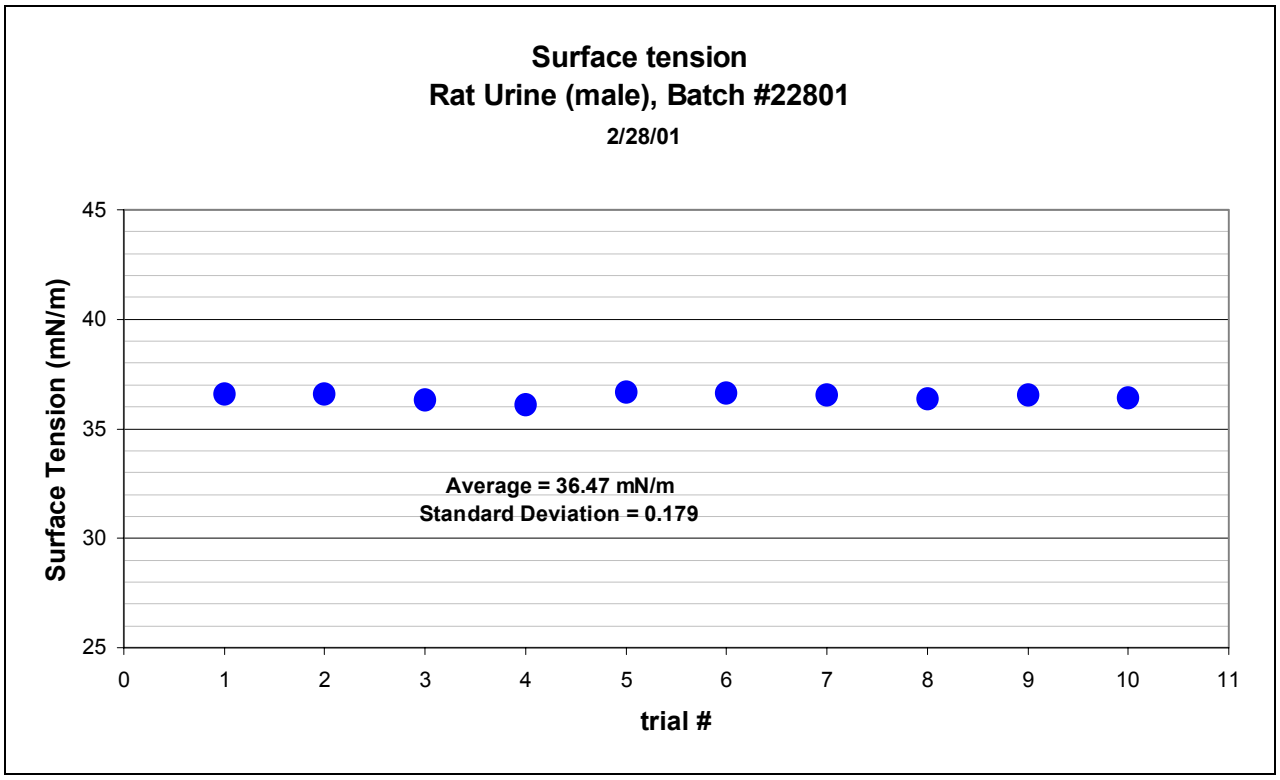

Figure 28: Surface tension of male rat urine at 23°C.

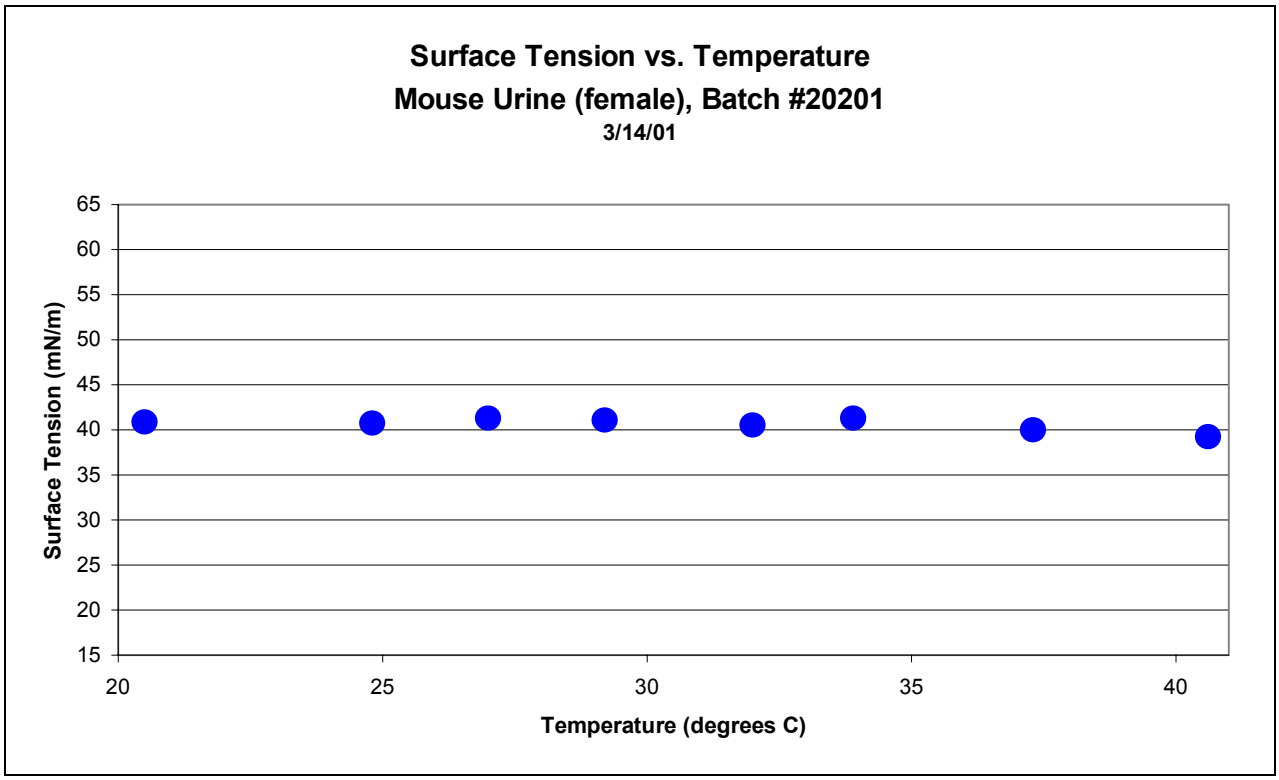

Figure 29: **Surface tension of mouse urine with temperature.**

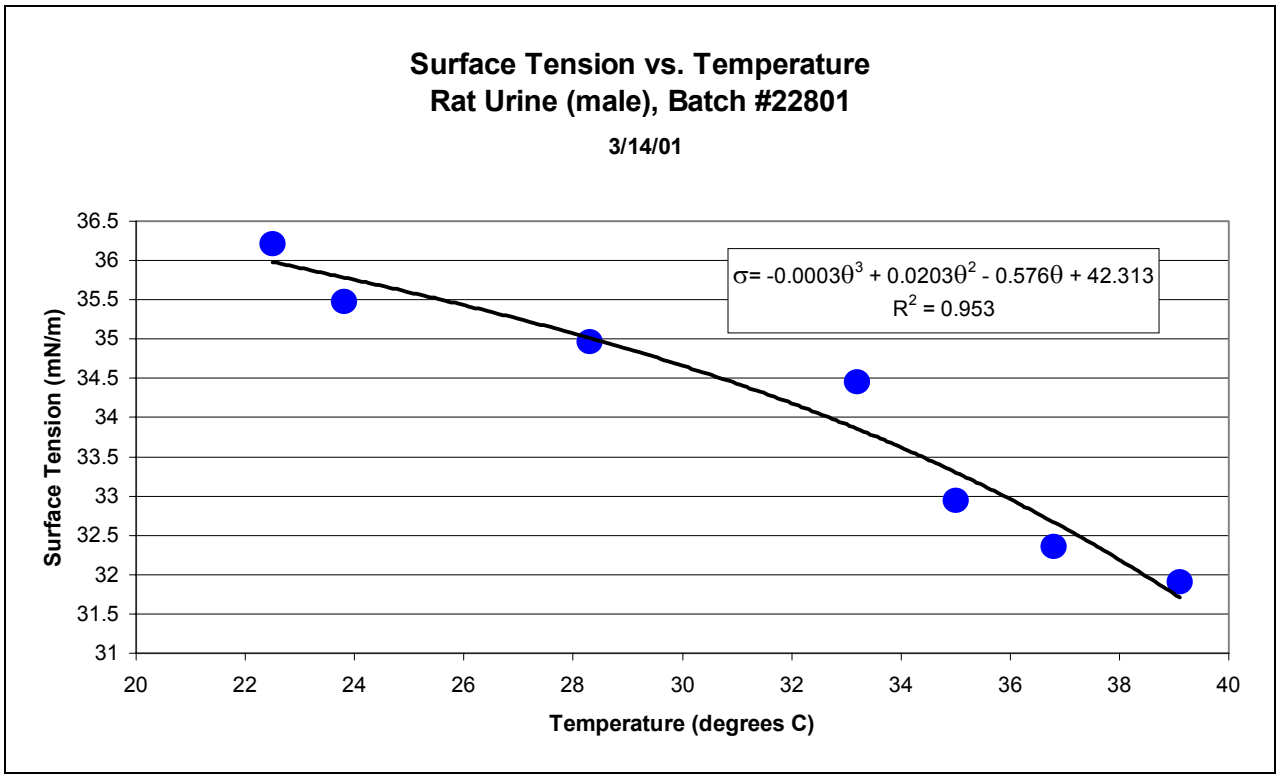

Figure 30: Surface tension of rat urine decreases with increasing temperature.

6.3. Analysis

To determine surface tension, data was manually calculated from the forces measured from the strain gage transducer on the Cahn DCA 315. The difference between software calculated data and our technique, shown in figure 22, is due to the choice of representative forces that determines surface tension at zero contact angles. We chose the force at zero depth of immersion (ZDOI) as opposed to the maximum force recorded by the strain gage because the maximum force might represent both the surface tension and elastic tension of non-Newtonian liquids. The surface tension of certain aqueous solutions with varying mass percents of solute revealed expected results. Sodium chloride increased the surface tension as more salt was added. Addition of urea decreased the surface tension of the solution while increased amounts of sucrose produced only small fluctuations in surface tension.

Surface tension measurements of mouse urine revealed the importance of filtration of each sample. Filtered and unfiltered mouse urines had surface tensions of 46.68 and 37.61 mN/m, respectively. Filtered rat urine had a lower surface tension at 36.47 mN/m.

The surface tension of Newtonian fluids is a function of temperature and concentration. Typically, surface tension decreases with increasing temperature. While the surface tension of the rat urine decreases with increasing temperature, the mouse urine merely fluctuates around an average value.

Overall uncertainty in measuring surface tension is due to the measurements of force, contact angle and perimeter in equation 6-1 was calculated to be ±0.25 mN/m. Error may also have occurred due to contamination of the platinum plate and liquid sample. In the examination of D.I.U.F. water, it is estimated that particulate contamination may cause up to ±5% error.

7. HYSTERESIS

7.1. Methods and Materials

7.1.1. *Wilhelmy Plate Method*

To determine the presence of hysteresis in contact angle, the same methods and materials used in section 6.1 were used with one exception. In addition to the platinum plate, a stainless steel plate was manufactured using two pieces of stainless steel foil (75mm width, 12.5mm thickness) adhered together. A piece was cut to approximately match the dimensions of the platinum plate.

7.1.2. *Sliding Droplet*

Hysteresis was also viewed by placing a large (>25μL) droplet of mouse urine on a stainless steel substrate attached to a rotating stage. The stage was rotated while a sequence of photographs was taken using an Optem Zoom 70 microscopic lens attached to a CCD camera module. The photographs were digitized using EPIX software.

7.2. Results

7.2.1. *Wilhelmy Plate Method*

There was obvious hysteresis for advancing and receding contact angles of both mouse and rat urine, according to figures 31-48. Variations include varying the speed of the motor/plate, purposely hitting the bottom of the container with the plate, dwelling in the liquid for 60 minutes, and repeating the normal cycle twice. Hysteresis was apparent in all cases.

Capillary numbers for the mouse and rat urine were calculated according to the equation,

$$Ca = \frac{\eta u}{\sigma} \qquad (7\text{-}1)$$

where η is the absolute viscosity, σ is the surface tension, and u is the velocity. For velocities of 80 and 264μm/s the capillary numbers are as follows:

Velocity	Rat Urine	Mouse Urine
80 μm/s	2.17×10^{-4}	2.02×10^{-4}
264μm/s	7.17×10^{-4}	6.66×10^{-4}

7.2.2. *Sliding Droplet*

The leading edge of the droplet had a visibly larger angle than the trailing edge. However, due to the angle at which the photographs were taken, contact angles could not be calculated accurately. A picture of the droplet, rotated to an angle just before the droplet begins to slide down the substrate, is shown later in figure 49. Animations of these droplets will also be provided with this report.

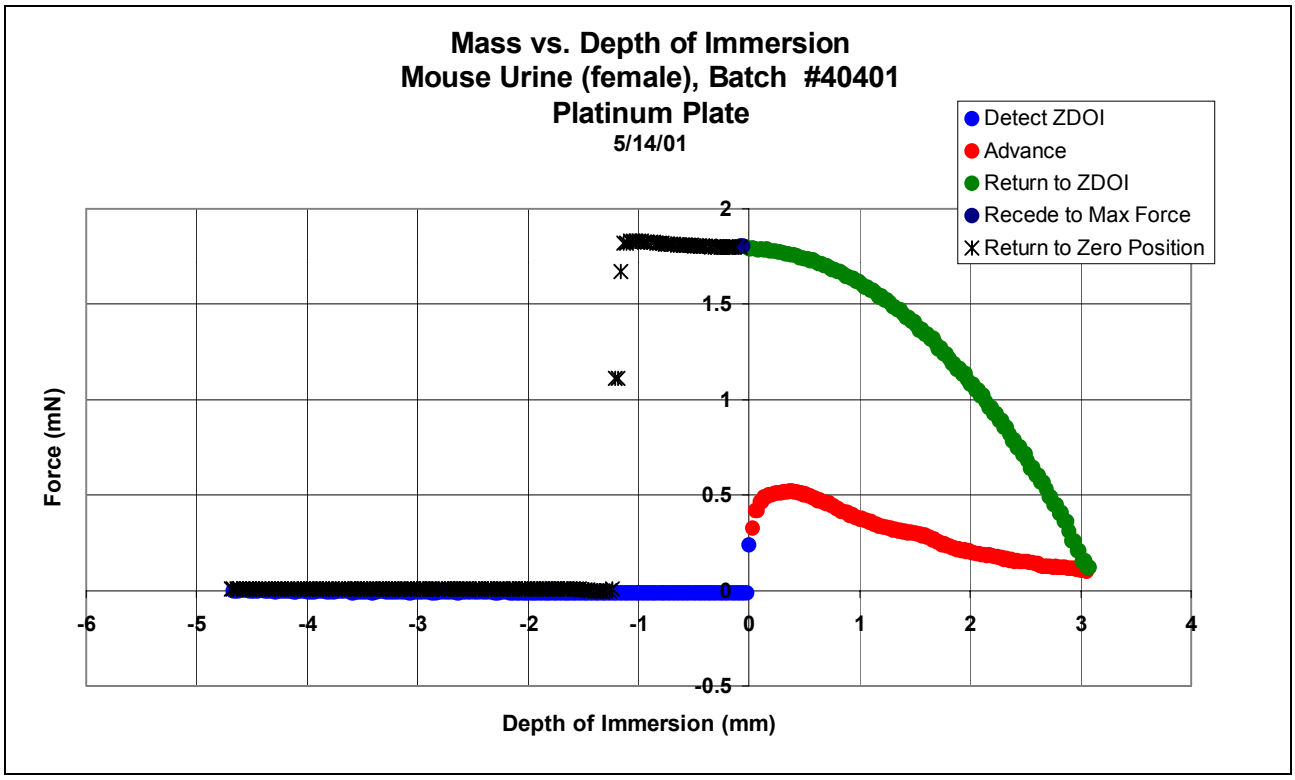

<u>Figure 31:</u> force vs. depth of immersion (female mouse urine). A platinum plate was used.

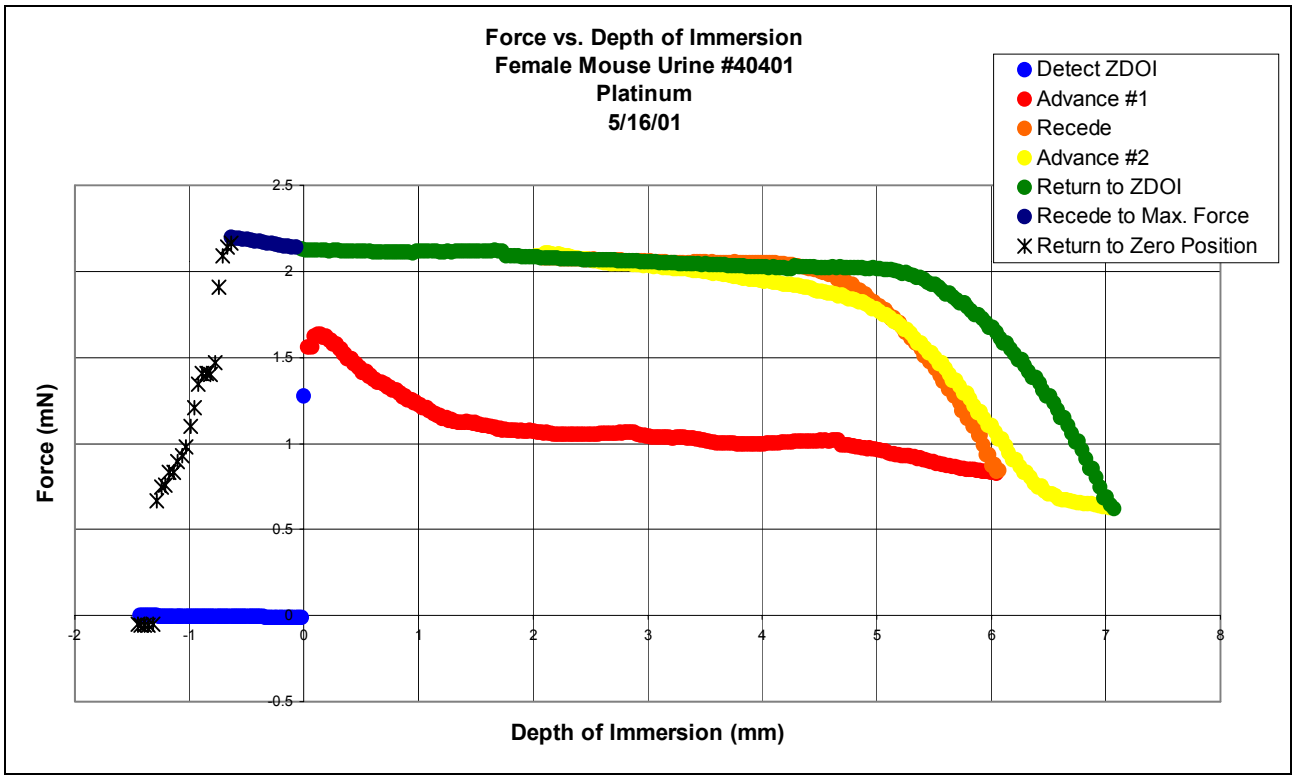

Figure 32: **Two-cycle force vs. depth of immersion (female mouse urine). A platinum plate was used.**

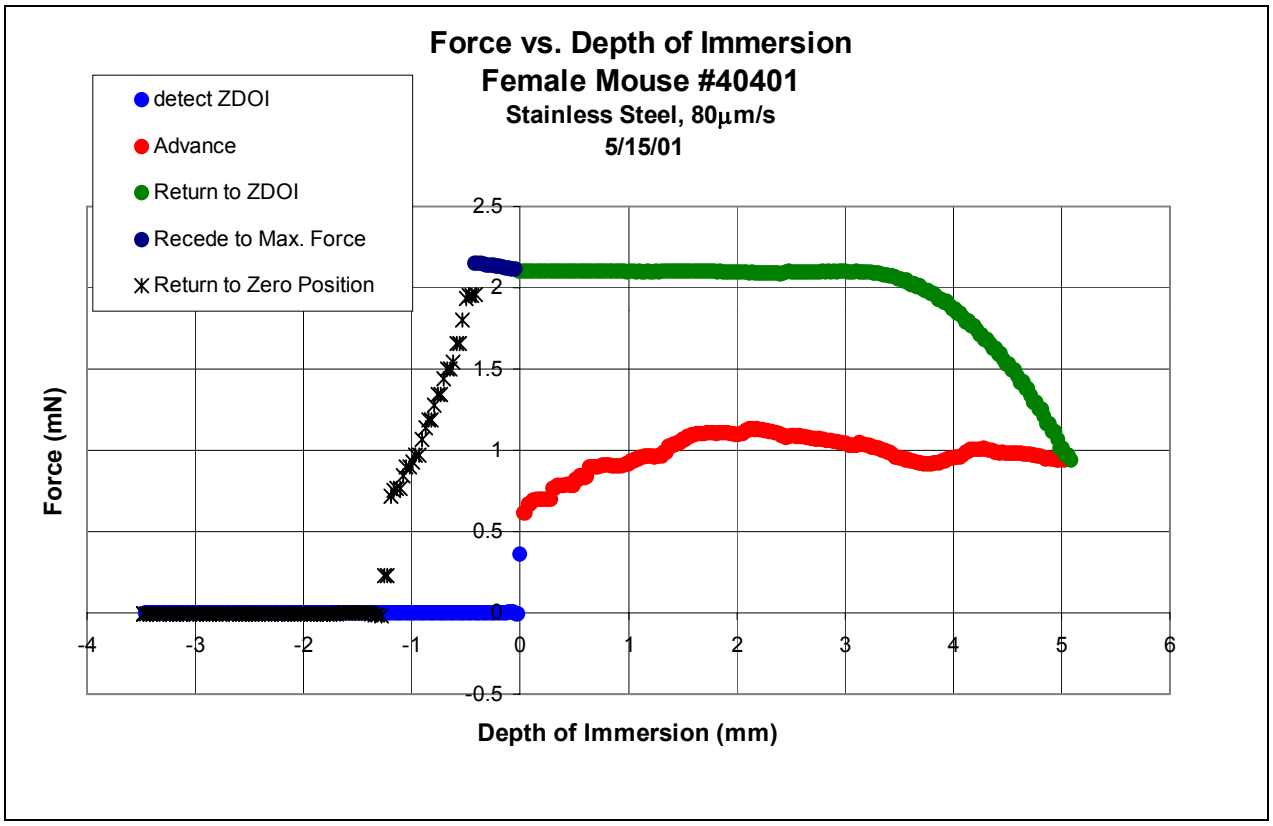

<u>Figure 33:</u> Force vs. depth graph (female mouse urine). A stainless steel plate was used.

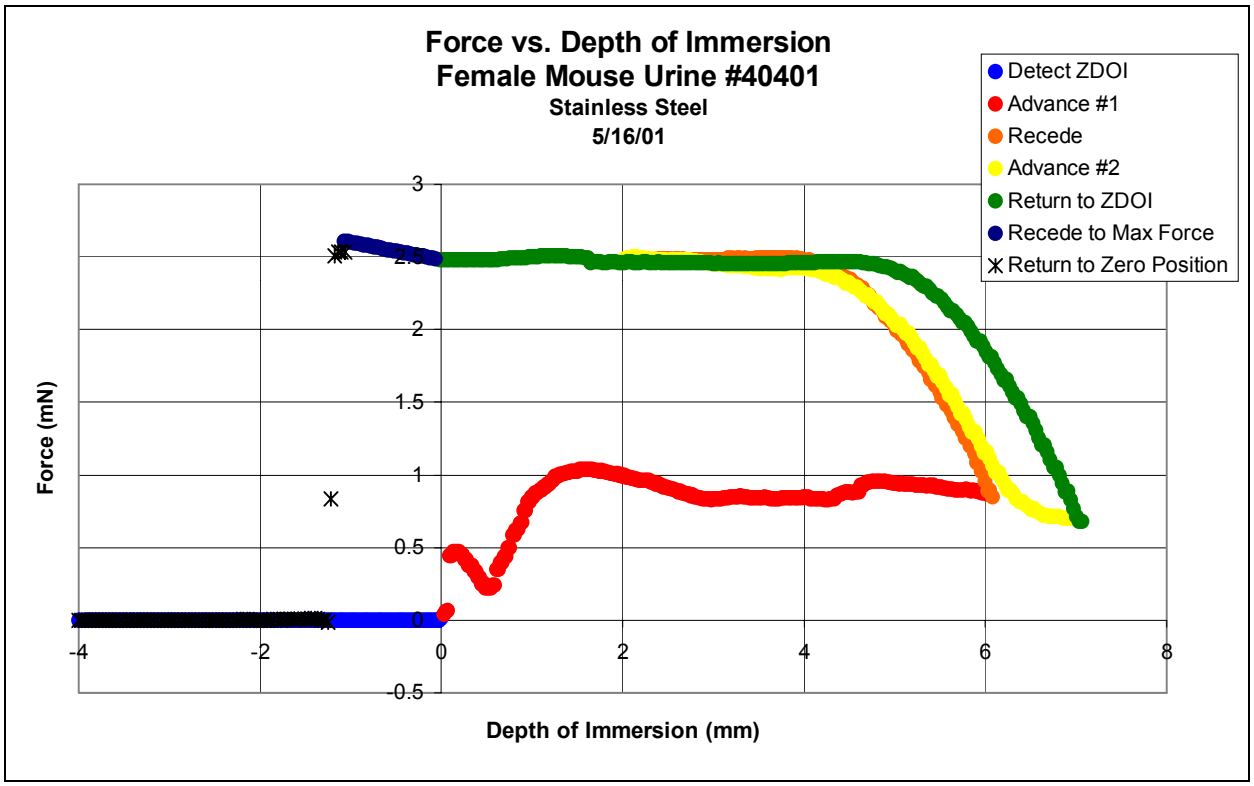

Figure 34: **Two-cycle force vs. depth of immersion (female mouse urine). A stainless steel plate was used.**

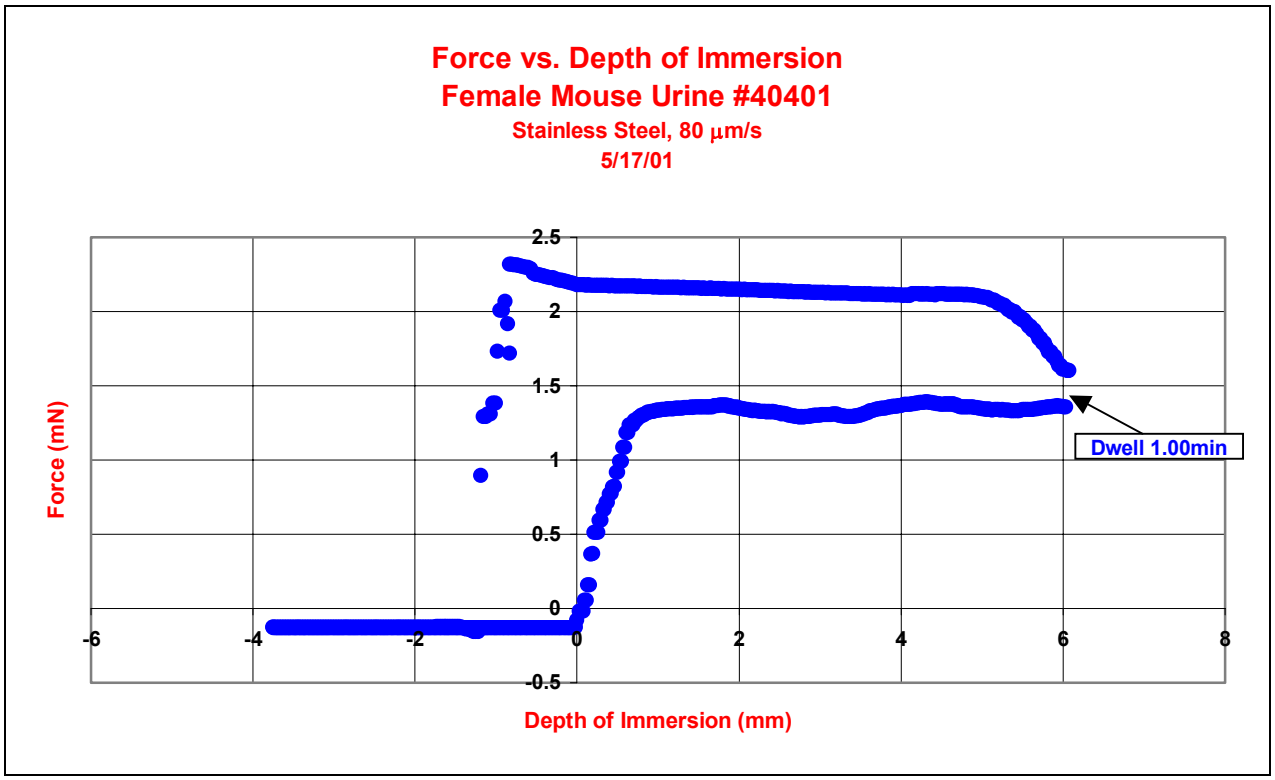

Figure 35: force vs. depth (female mouse urine). After advancing, the plate was programmed to dwell for 60 seconds. A stainless steel plate was used. Automatic tare was not used.

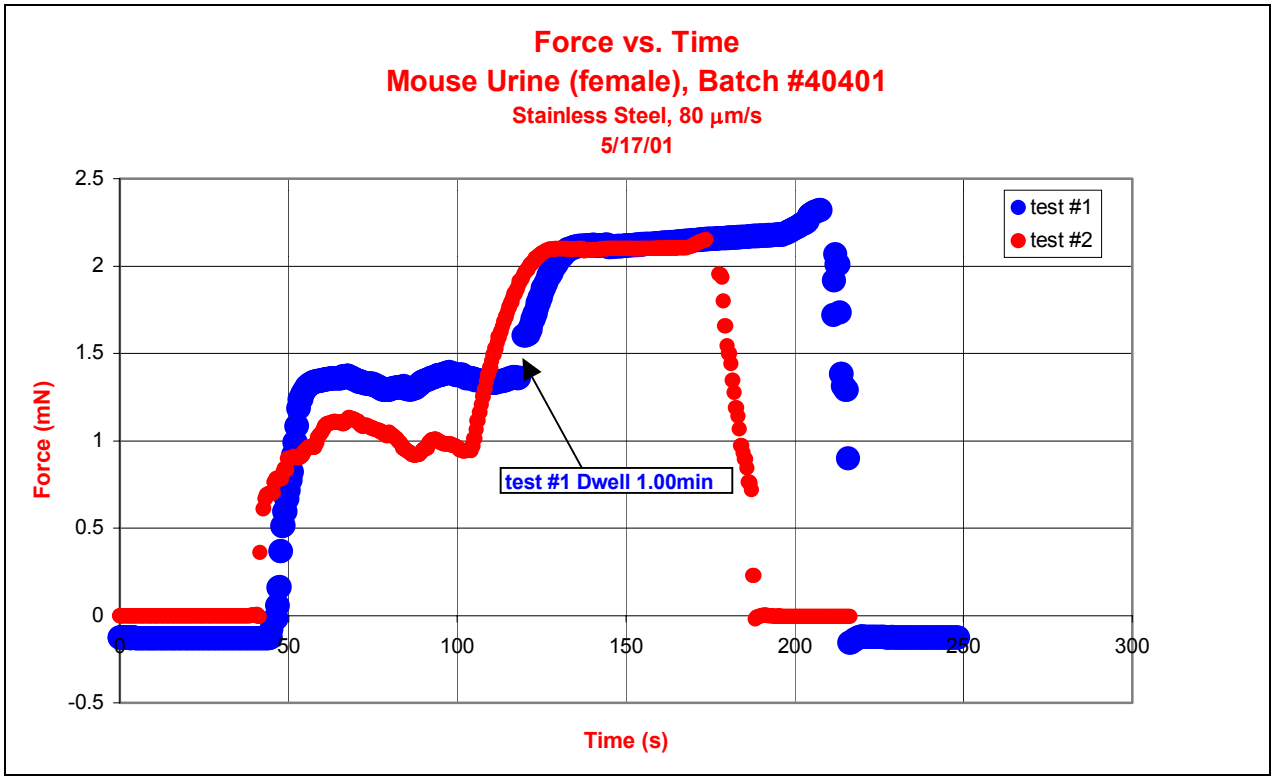

Figure 36: force vs. time (female mouse urine). A stainless steel plate was used. This graph shows reproducibility with the overlap of two tests.

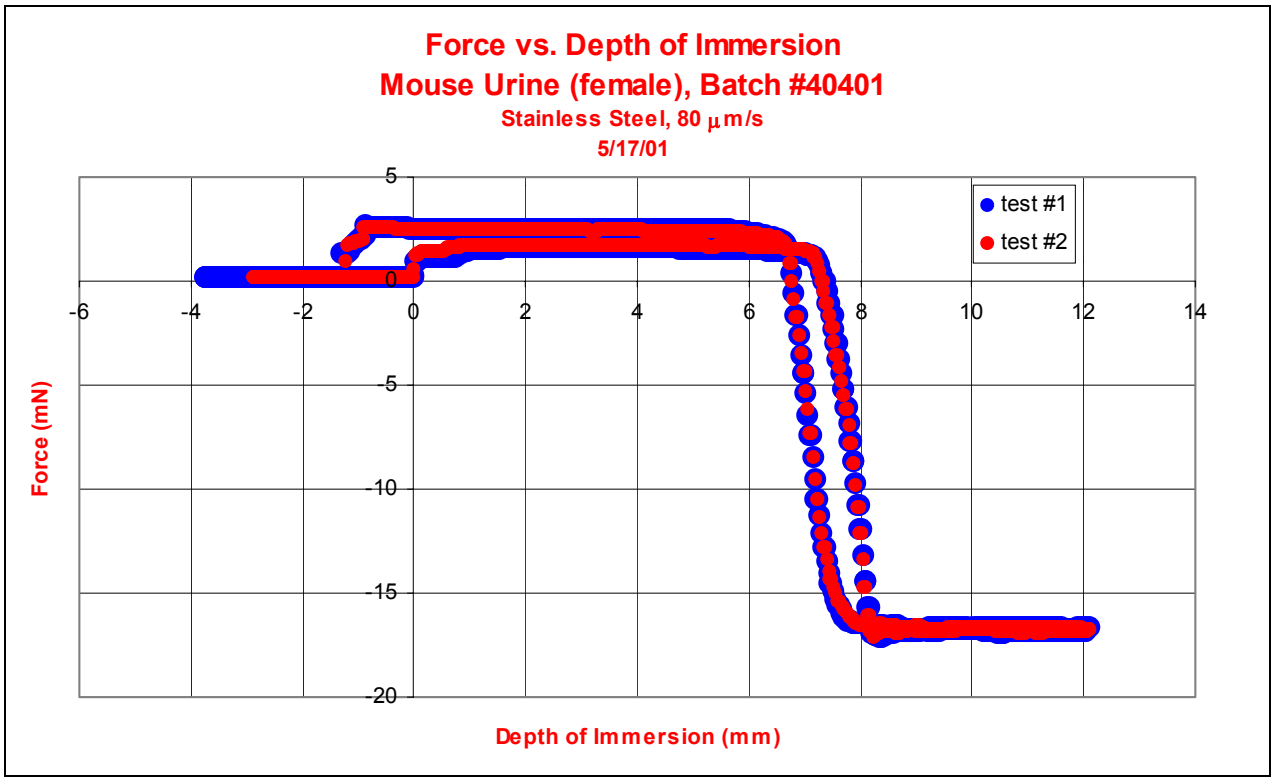

<u>Figure 37:</u> Force vs. depth of immersion (female mouse urine). A stainless steel plate was programmed to hit the bottom of the container. Automatic tare was not used.

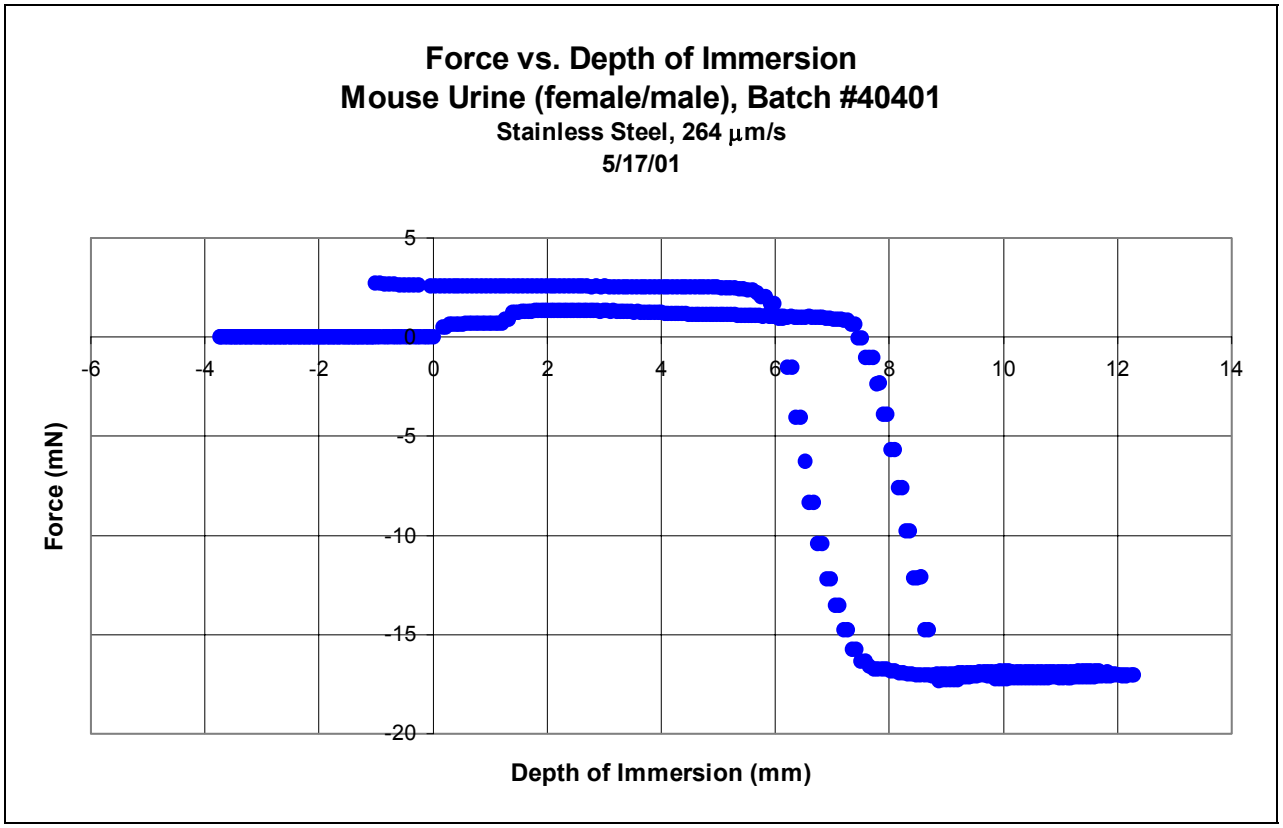

<u>Figure 38:</u> Force vs. depth of immersion (female/male mouse urine). A stainless steel plate is used at a velocity of 264 μm/s. The probe is programmed to hit the bottom of the container and dwell for 60 seconds. Automatic tare was not used.

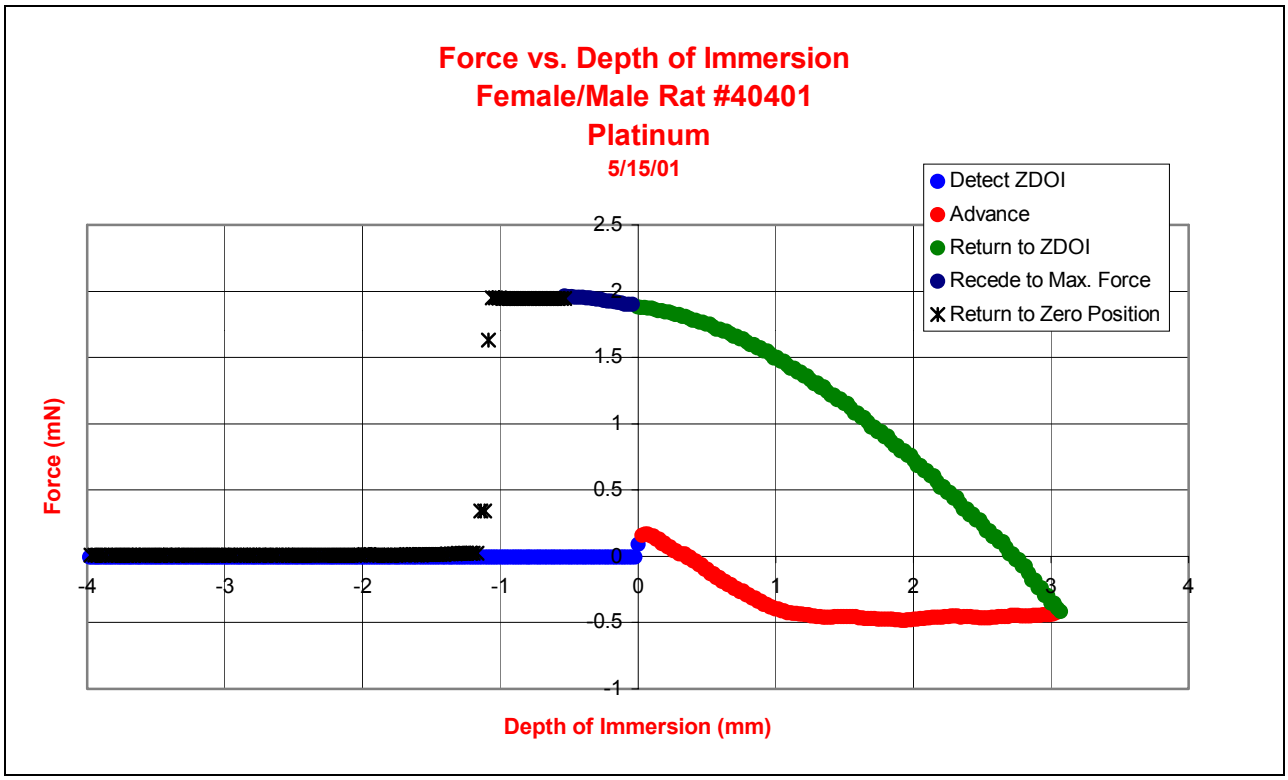

<u>Figure 39:</u> force vs. depth of immersion (female/male rat urine). Platinum plate used.

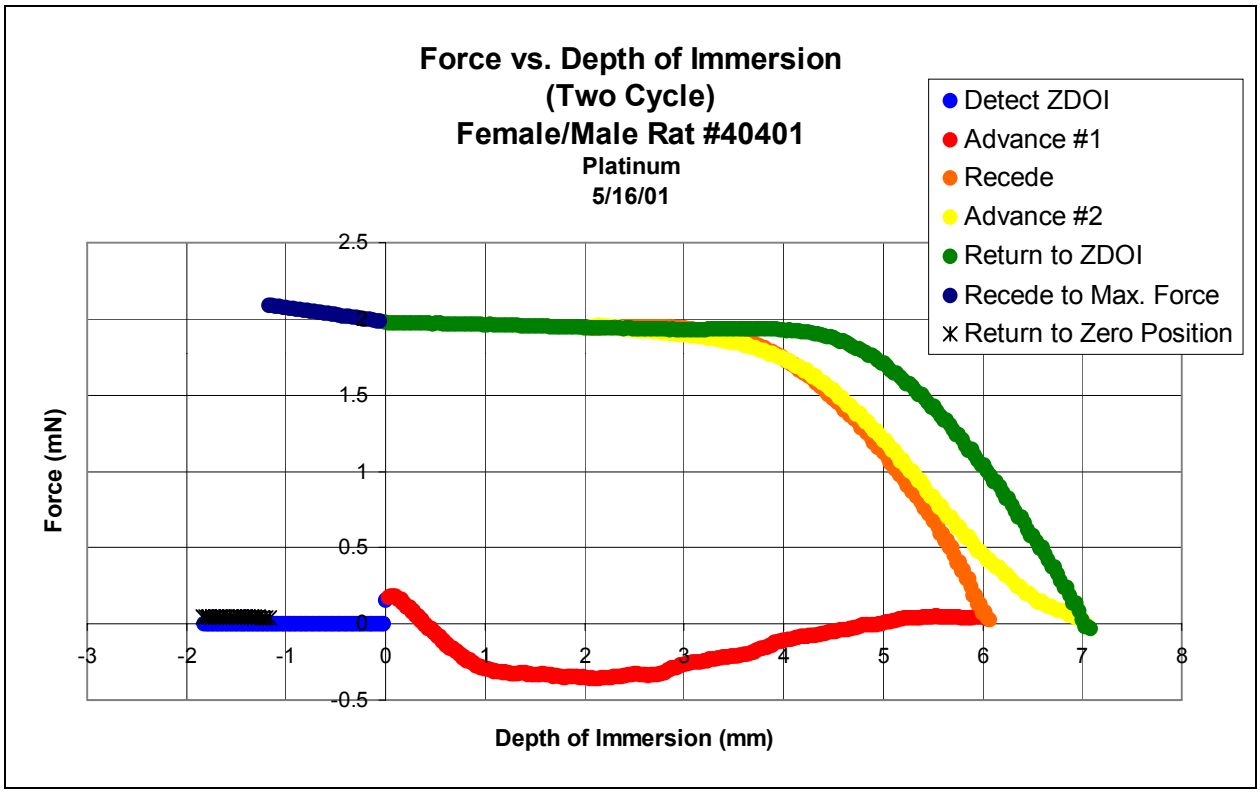

Figure 40: **Two-cycle force vs. depth of immersion (female/male) rat urine. A platinum plate was used.**

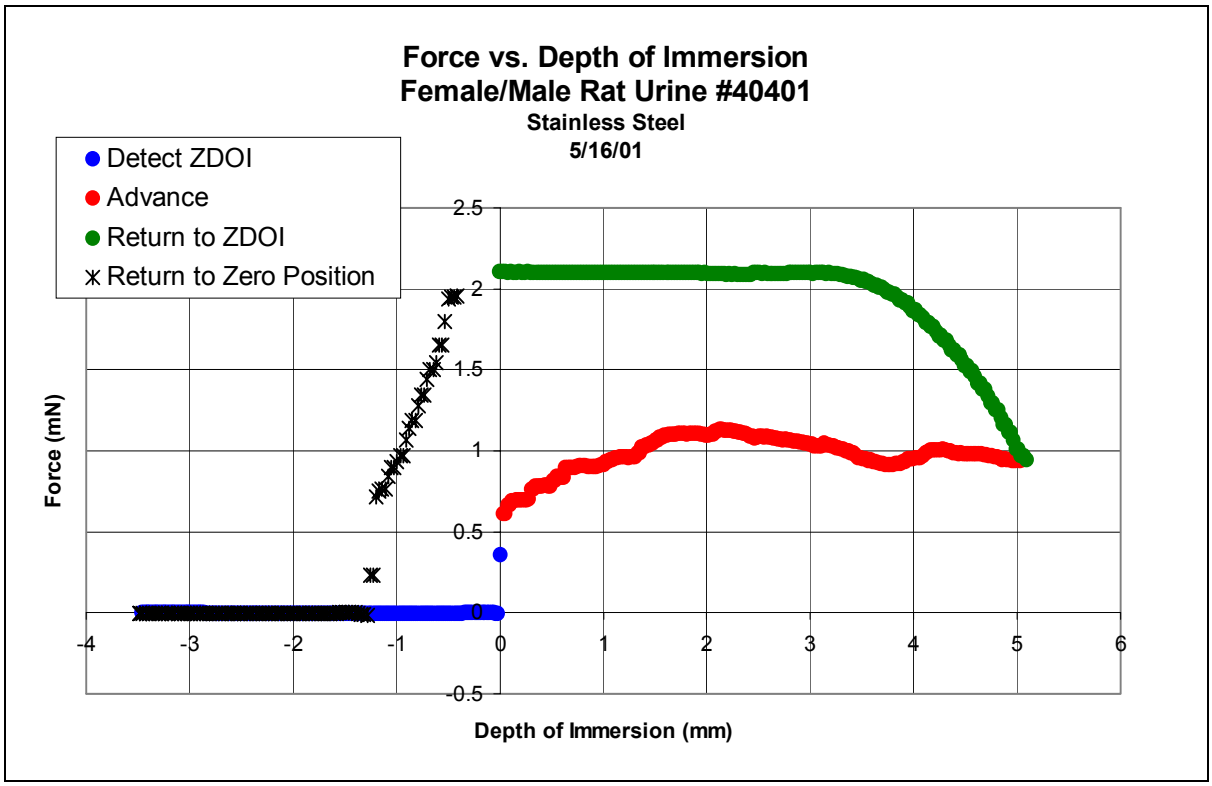

Figure 41: **Force vs. depth of immersion (female/male rat urine). Stainless steel plate used.**

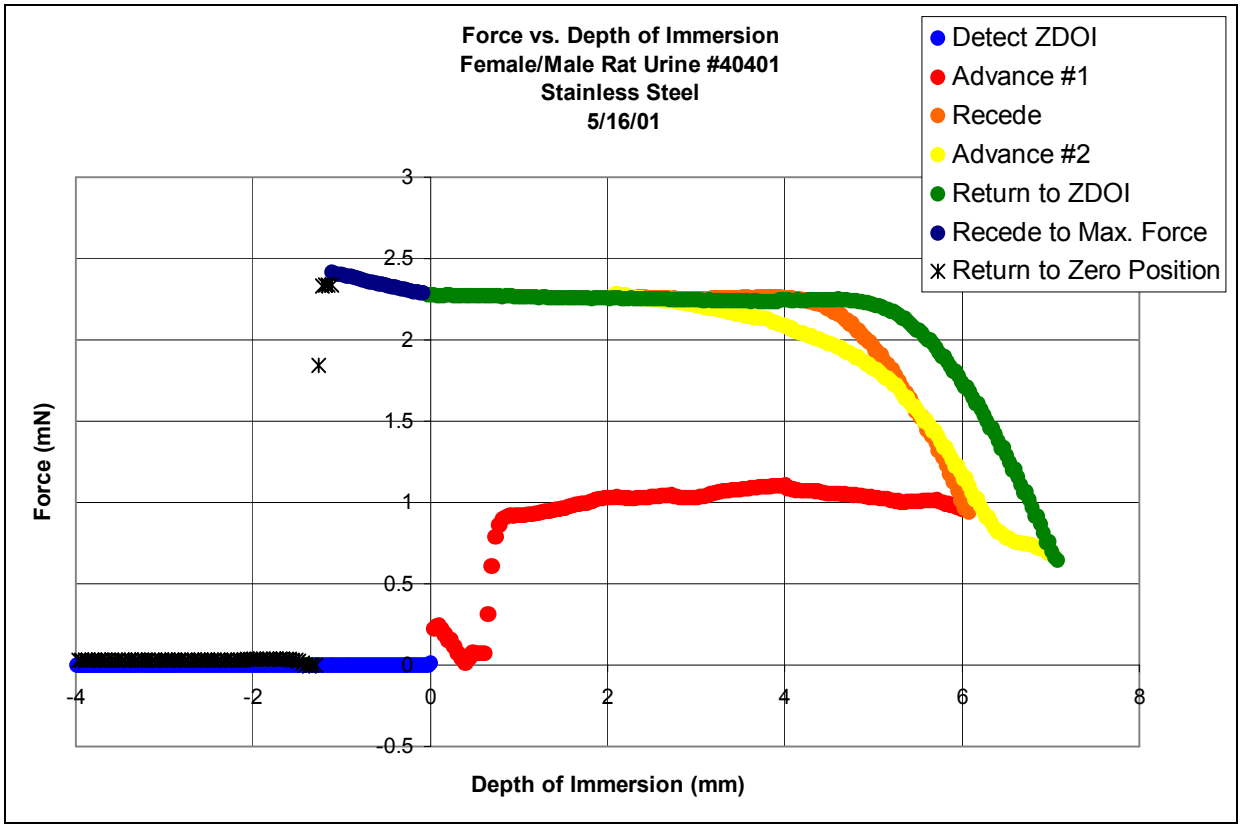

Figure 42: **Two-cycle force vs. depth of immersion (female/male rat urine). A stainless steel plate was used.**

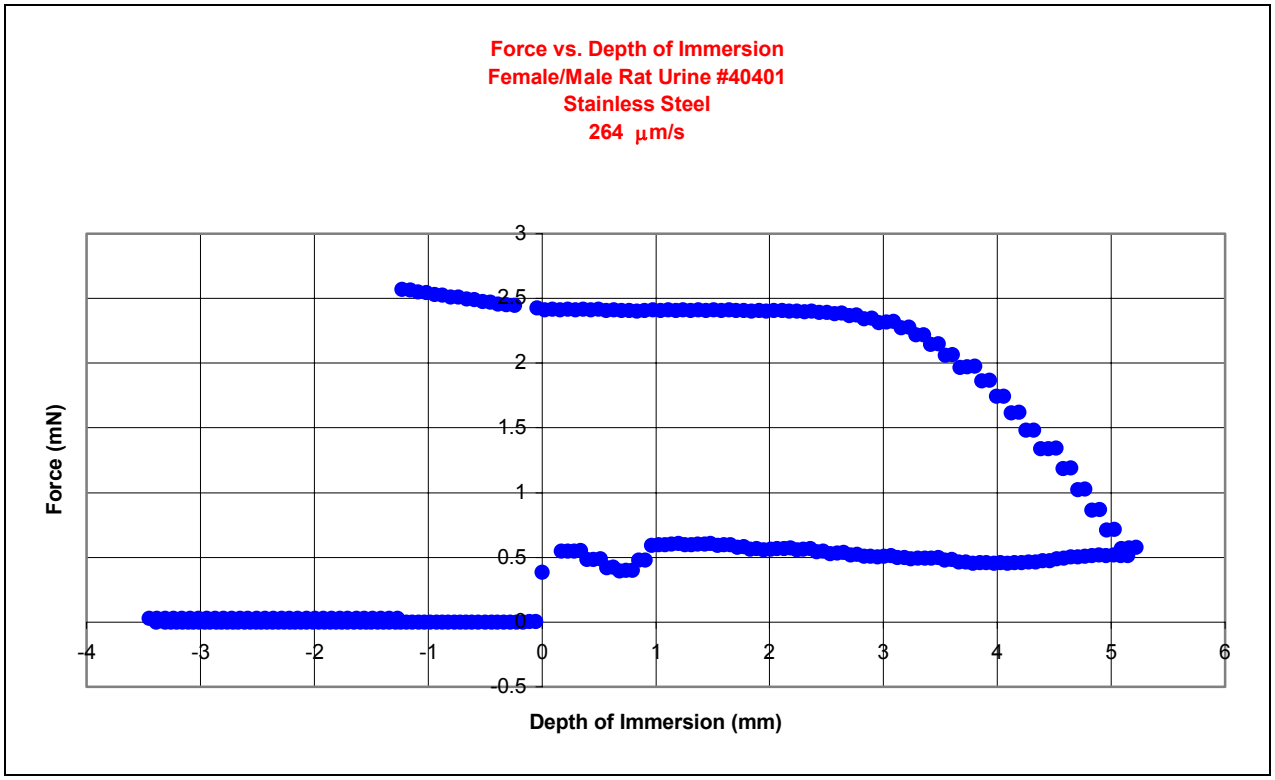

Figure 43: **force vs. depth of immersion (female/male rat urine). A stainless steel plate was immersed at a velocity of 264 µm/s.**

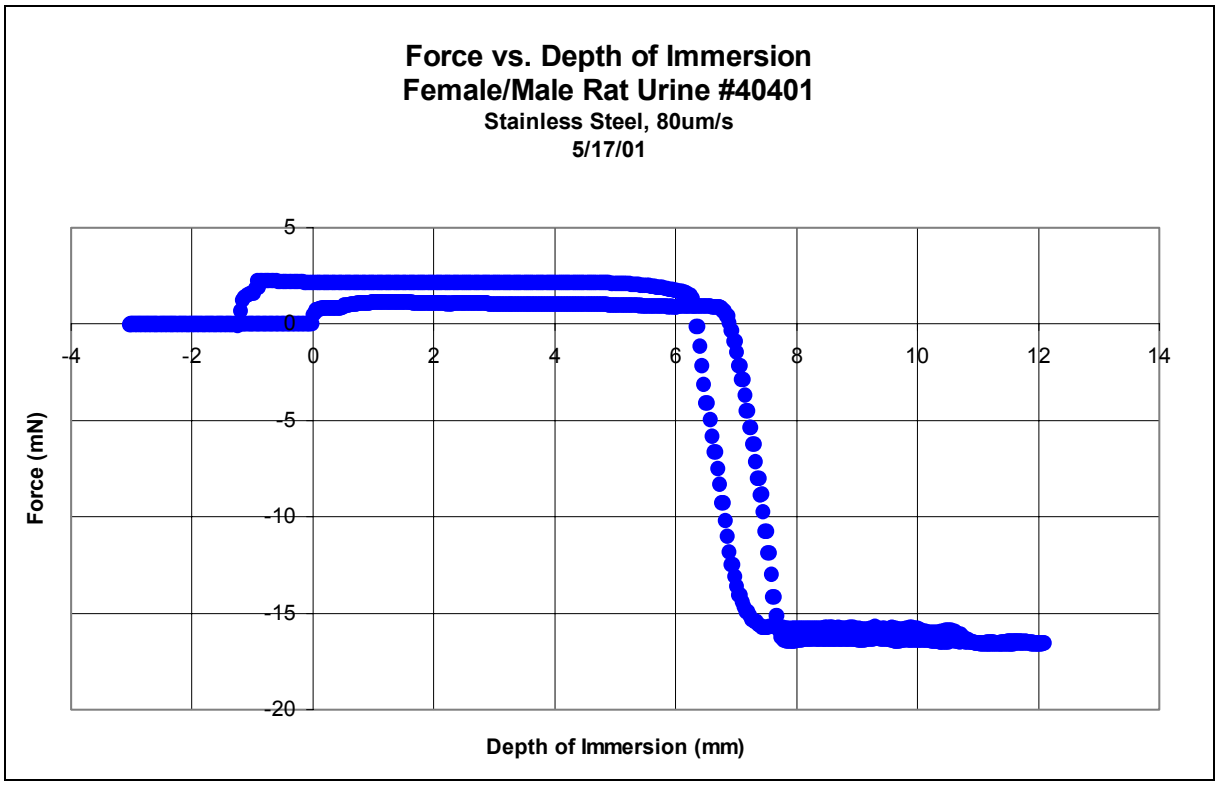

Figure 44: **force vs. depth of immersion (female/male rat urine). A stainless steel plate was programmed to hit the bottom of the container and dwell for 60 seconds.**

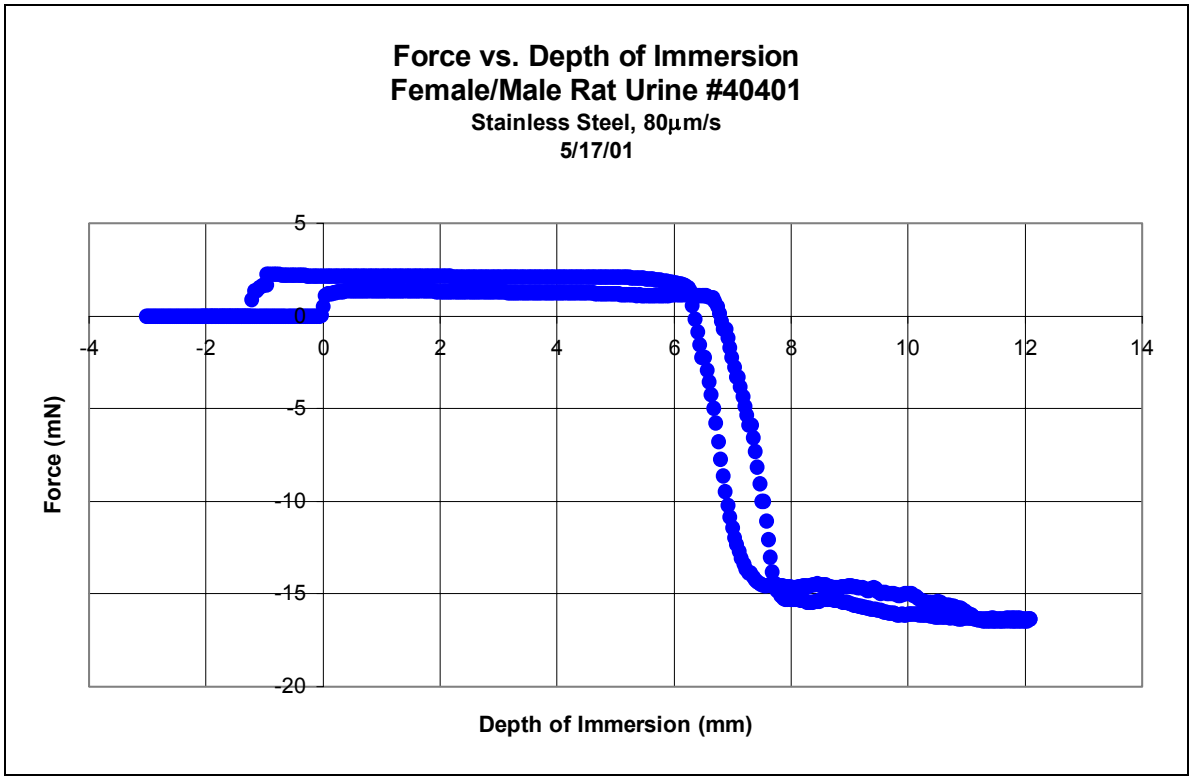

Figure 45: force vs. depth of immersion (female/male rat urine). A stainless steel plate was programmed to hit the bottom of the container and dwell for 60 seconds. Automatic tare was not used.

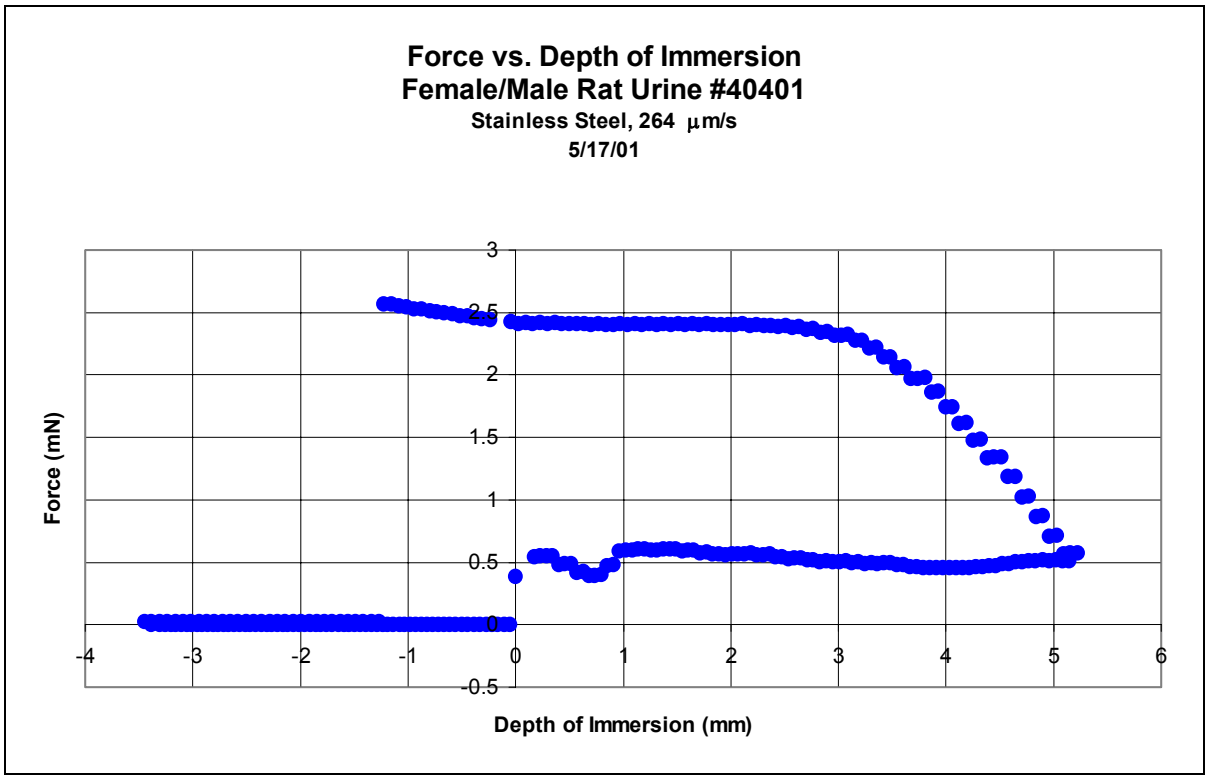

Figure 46: force vs. depth of immersion (female/male rat urine). A stainless steel plate was immersed at a velocity of 264 µm/s.

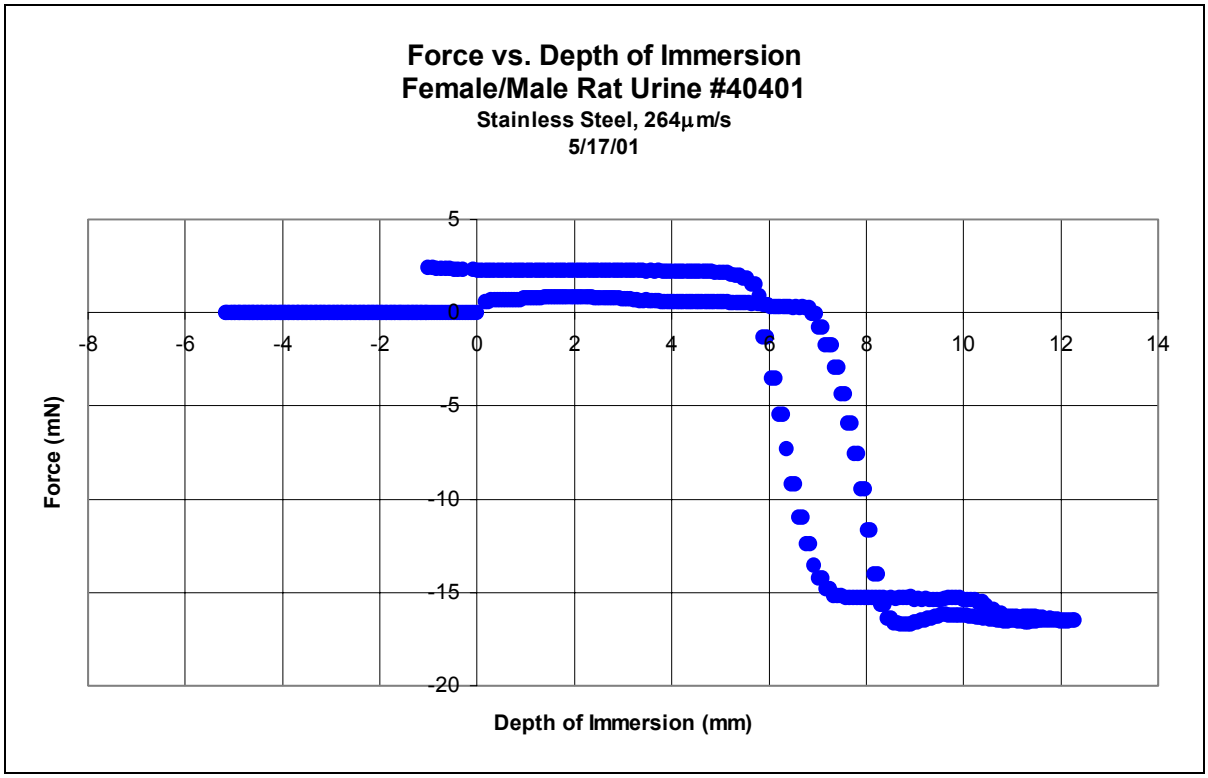

Figure 47: **force vs. depth of immersion (female/male rat urine). A stainless steel plate was immersed at a velocity of 264 µm/s. The plate was programmed to hit the bottom of the container and dwell for 60 seconds.**

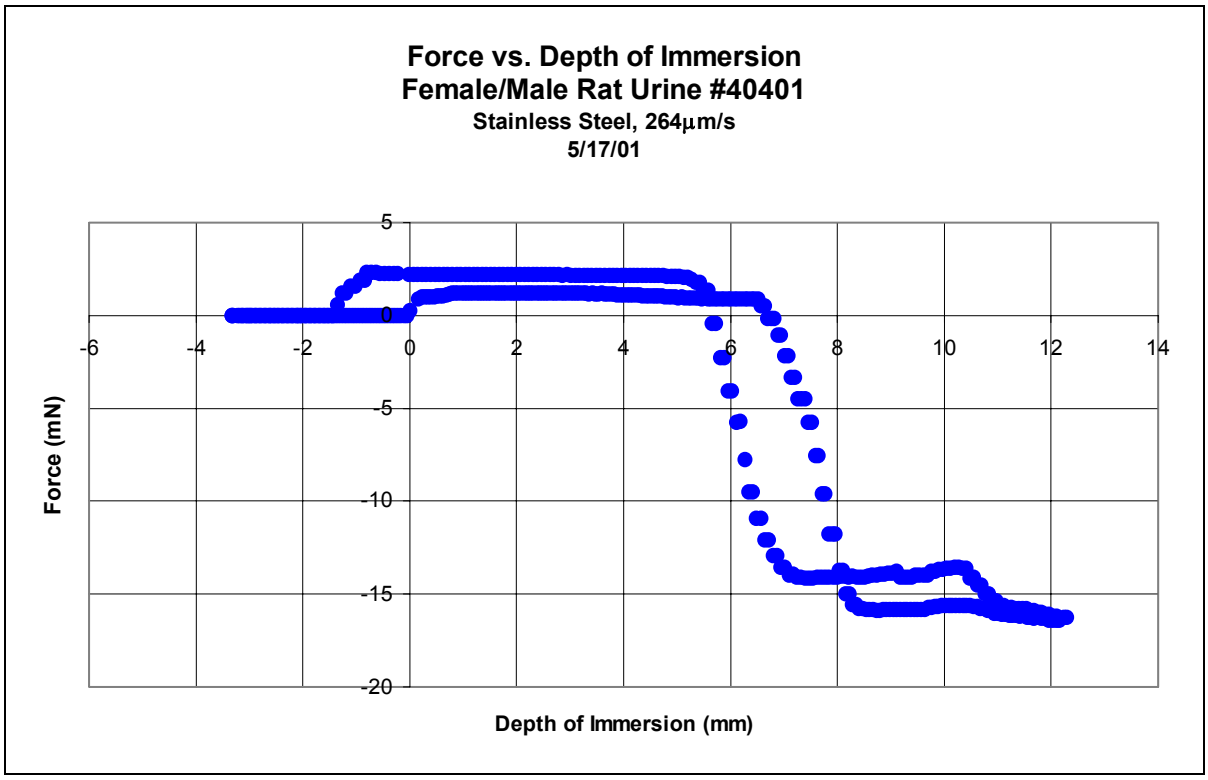

Figure 48: **force vs. depth of immersion (female/male rat urine). A stainless steel plate was immersed at a velocity of 264 µm/s. The plate was programmed to hit the bottom of the container and dwell for 60 seconds. Automatic tare was not used.**

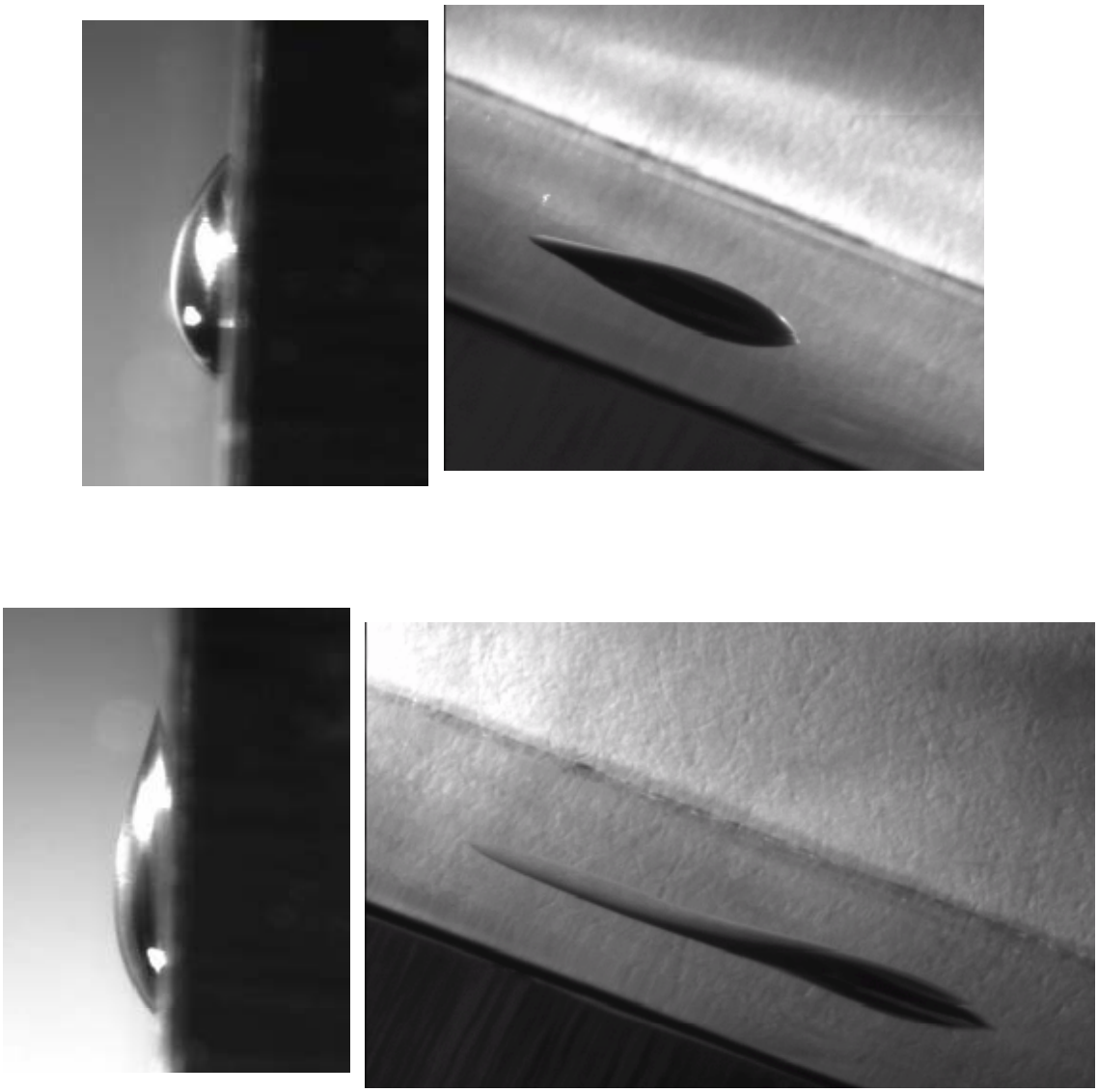

<u>Figure 49</u> Clockwise from top left: 5µL droplet of mouse urine at 90°, 25µL droplet at 45°, 25 µL of rat urine at 45°, and 5µL of rat urine at 90°. Batch #40401 on stainless steel substrate.

7.3. Analysis

The force versus depth of immersion graphs show a force hysteresis. Since the surface tension is constant at a particular temperature and concentration, one might conclude these differences are due to changes in advancing and receding contact angles. To rule out hysteresis caused by method, different procedures were used which correspond to each graph in the above section.

It was also observed that because the capillary numbers are much less than one, the liquid tends to creep up the plate upon immersion as well as withdrawal from the urine. According to equation 7-1, the only variable is u, the velocity of the plate. In attempts to increase the capillary number, the velocity was also increased, but the limitations of the DCA 315 motor made it impossible to increase the velocity greater than 264μm/s.

In the experiment where a droplet of urine was placed on a stainless steel substrate, hysteresis was determined to be a function of drop volume. A 5μL droplet of urine can be rotated at a 90° angle with no visible hysteresis, while a larger 25μL shows obvious differences between leading and trailing contact angles when rotated at approximately 45°.

Error described for the DCA 315 in section 6.3 is also applicable in this case, as the same methods were used. On top of these, the self-made stainless steel plate had visible imperfections, which were impossible to resolve. For this reason, we were unable to calculate a reliable contact angle using this method. In the subsequent section, a more accurate method is presented.

8. CONTACT ANGLE

8.1. Materials and Methods

Stainless steel foil was adhered to a lab jack and a 5μL droplet was placed onto the surface. To measure the contact angle of rat and mouse urine, pictures of the droplets were taken using an Optem Zoom 70XL (#29-96-91) lens and threaded TV tube (#29-90-72) attached to a Sony XC-75 CCD video camera module. The photographs were digitized using EPIX software. A plot of the outline of each droplet was produced by one of the following methods. The contact angle was determined by measuring the angle between the horizontal and tangent to the outermost edge of the droplet.

8.1.1. *Manual Determination of Droplet Profile*

The digitized images were viewed in Microsoft Imaging® software and pixel coordinates of the outer edge of the droplet were determined using a "point and click" method (e.g. a pixel was selected with a mouse and pixel coordinates were displayed on the screen). These pixel coordinates were converted to Cartesian coordinates in Microsoft Excel®.

8.1.2. *Automated Determination of Droplet Profile*

Digitized images were processed using Matlab® to produce outlines of the droplets. The coordinates produced by Matlab® were imported into Microsoft Excel®.

8.2. Results

The contact angles of mouse urine on stainless steel resulting from manual and automated methods were 47.25 and 45.53 degrees, respectively. These results are shown in figures 50-53. The contact angle of rat urine on stainless steel calculated from an automated profile was 45.41 degrees, as seen in figures 54-55. The resolution was 153 pixels/mm.

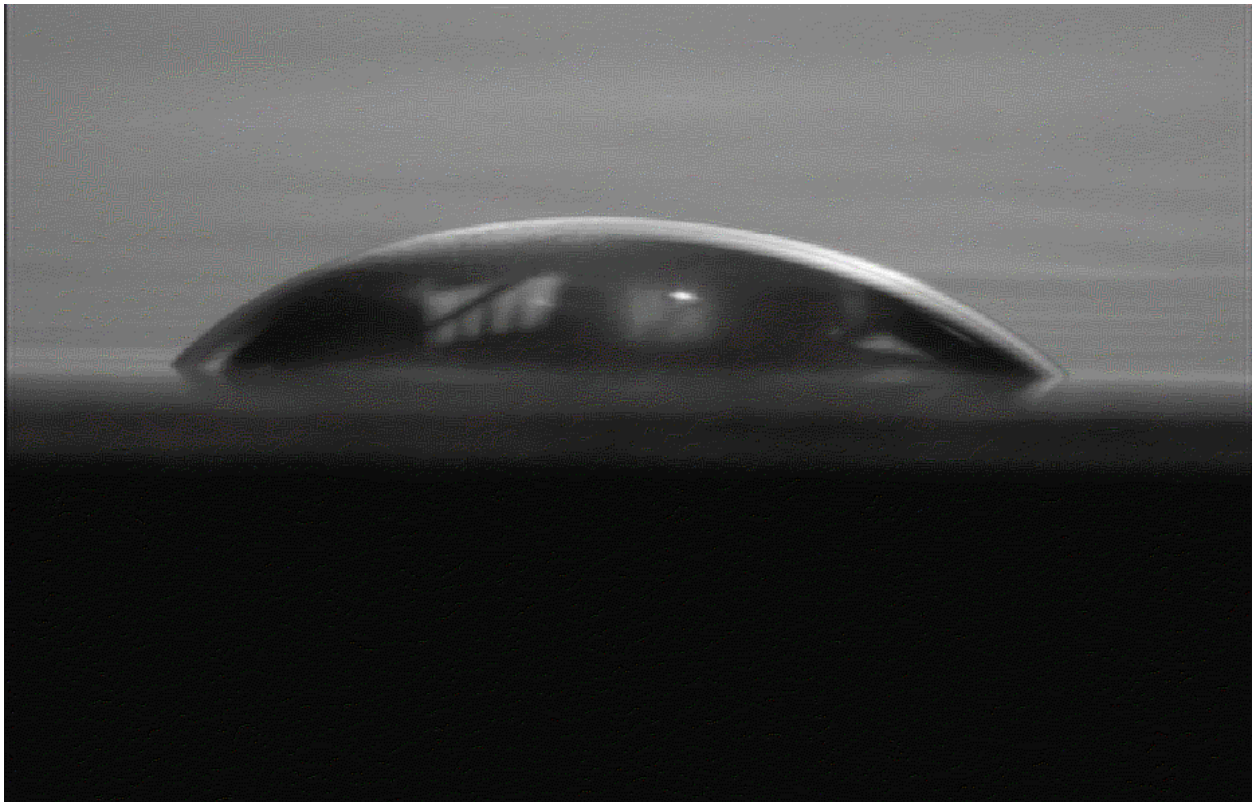

Figure 50: **Photograph of male mouse urine batch #40401. 4/09/01**

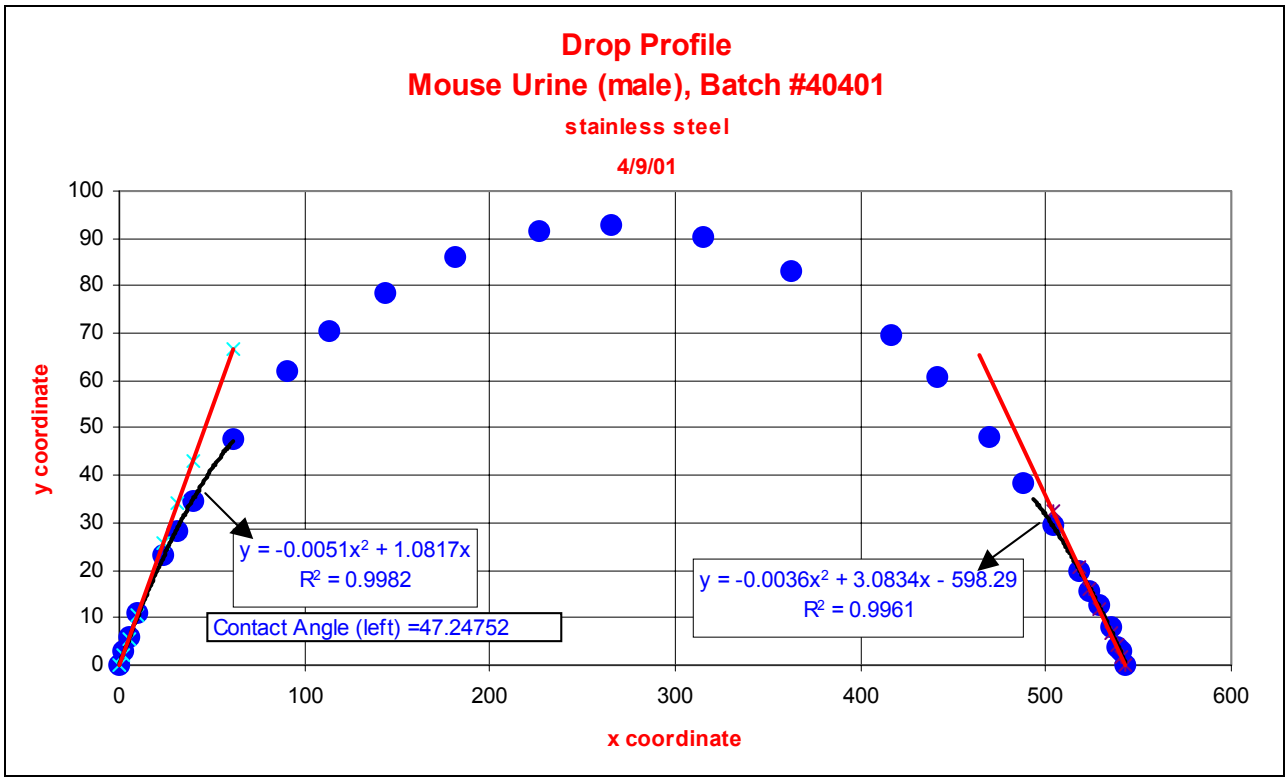

Figure 51: **Drop profile of male mouse urine, batch #40401. Produced manually.**

Figure 52: Photograph of a 5μL male mouse urine on a stainless steel substrate (x50), batch #40401. 4/11/01

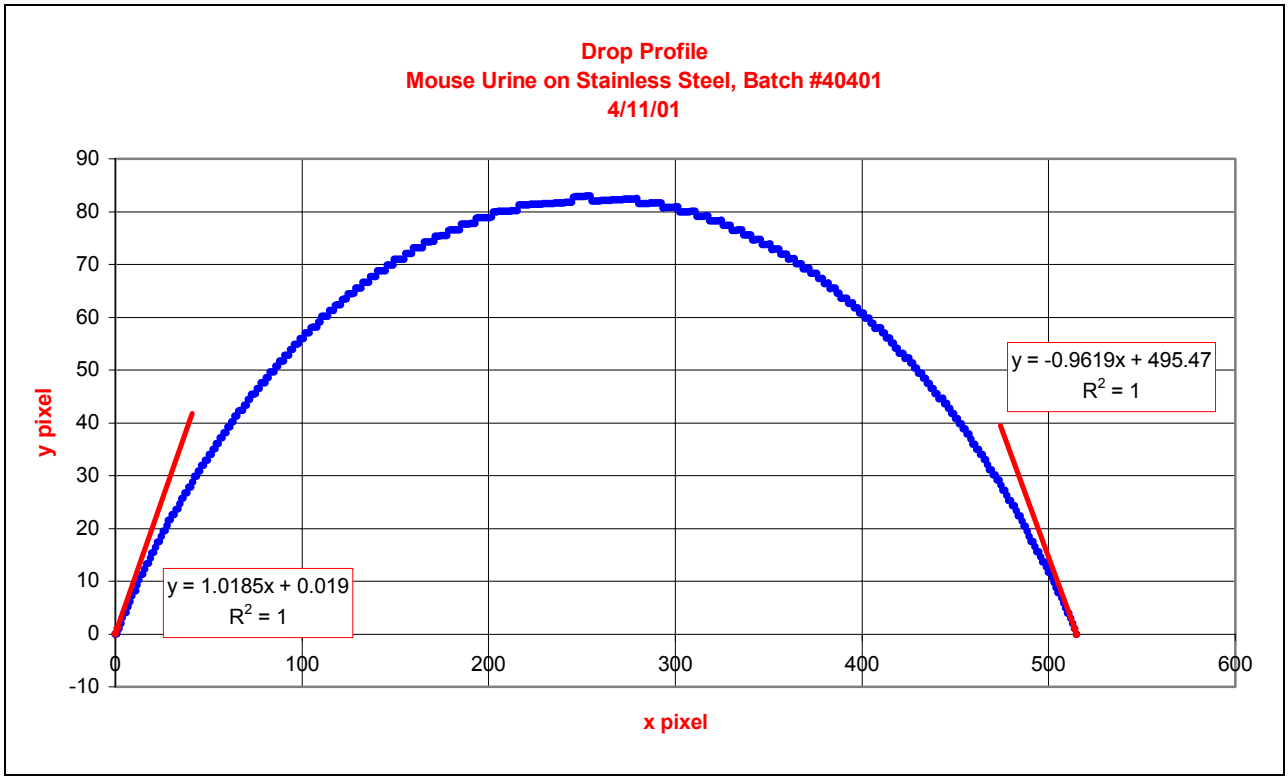

Figure 53: Drop profile of 5μL of male mouse urine. Produced using Matlab®.

<u>Figure 54:</u> Photograph of a 5μL droplet of male rat urine on a stainless steel substrate (x50), batch #40401.

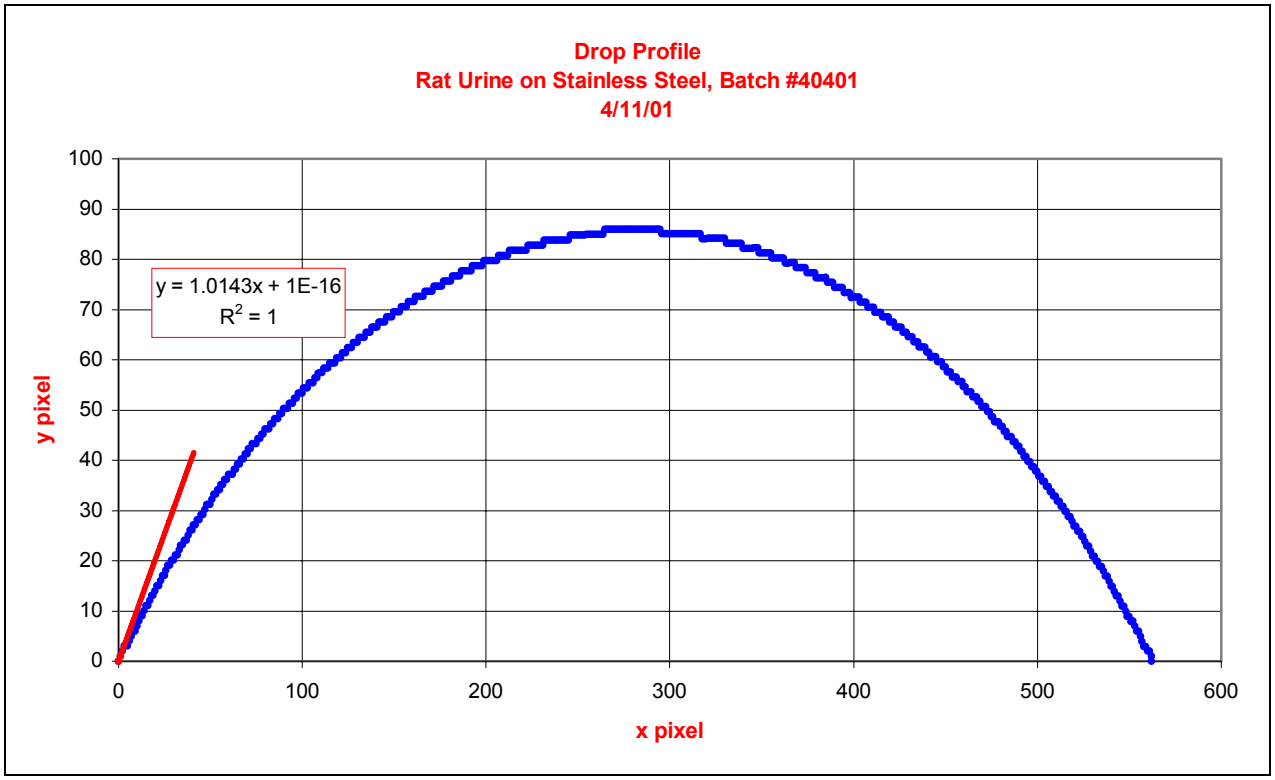

Figure 55: Droplet profile of male rat urine, batch #40401. Produced using Matlab®.

8.3. Analysis

Contact angles for the mouse and rat urine on stainless steel substrates were 45.53 and 45.41, respectively. The major contributor to overall uncertainty in the contact angle measurements was graphical error. Accuracy of the contact angle was determined by the image resolution.

9. EVAPORATION RATE

9.1. Methods and Materials

A small glass container was placed on a Thomas Scientific T200S digital balance. The balance was zeroed and an arbitrary volume of mouse urine was placed in the container. The initial weight of the urine was recorded. The urine was left to evaporate in a room averaging 23.0% relative humidity and 23.0°C. The mass of the urine was recorded at approximately 30-minute intervals. Relative humidity and temperature were recorded using an Extec Instruments Humidity/Temperature meter.

9.2. Results

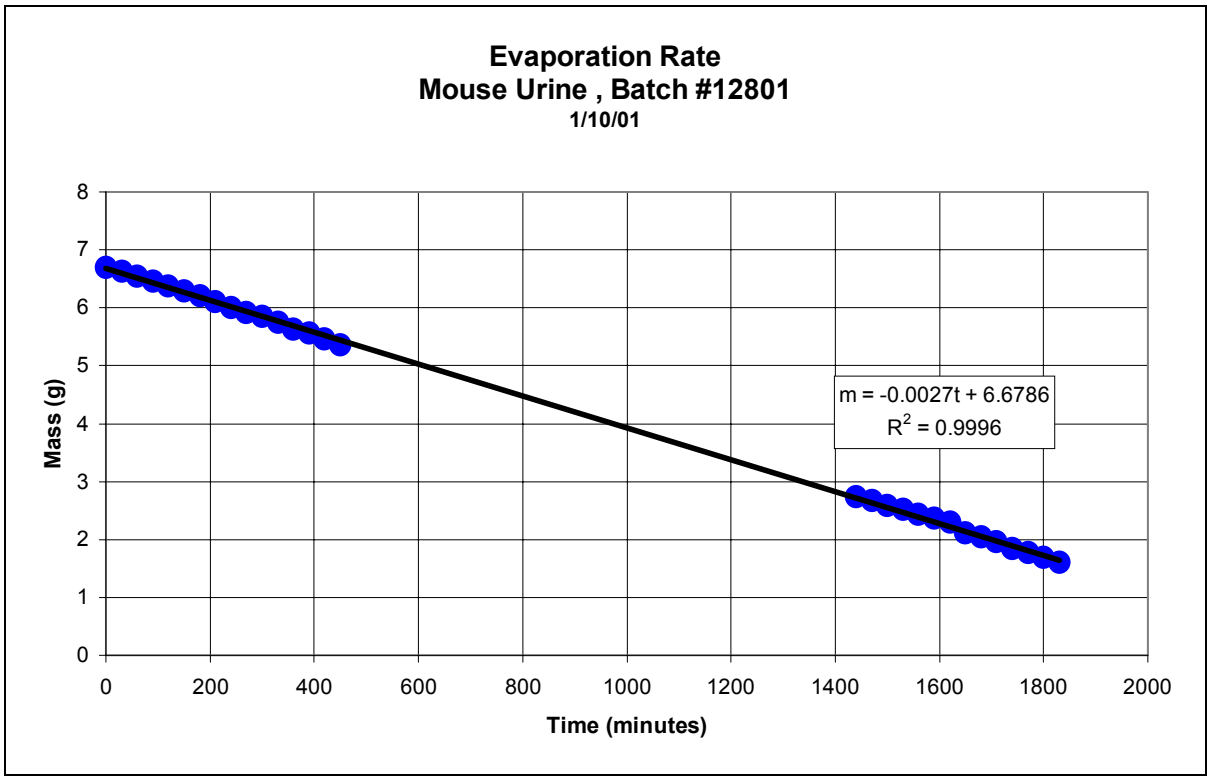

Figure 56: Evaporation rate of mouse urine.

9.3. Analysis

The urine evaporated linearly over time for the duration measured in figure 56. The absences of data points in the center of the graph were due to continuation of the experiment over-night. The liquid evaporates at a rate of about 3 mg/min. Further experiments may be necessary to determine the evaporation rate as a function of ambient temperature and humidity.

10. CONCLUSION

The densities of the both urines were approximately that of water. The results show, rat urine was slightly less dense than mouse urine.

Reverse-flow viscometer tubes were used to determine the kinematic viscosities of rat and mouse urine. The viscosity of both urines increased as it was cooled from body temperature (37°) to room temperature (23°C). The viscosity of the mouse urine changed at a slightly higher degree with respect to temperature at 0.02 cSt/°C. At room temperature the kinematic viscosity of mouse urine was 1.12 cSt and therefore more viscous than rat urine which had a viscosity of 0.99cSt.

The surface tension of the rat urine was inversely related to the temperature. As the urine cooled, the surface tension increased approximately along the line of a third-order polynomial. On the other hand, even when cooled, mouse urine fluctuated about an average value of 40.64 dynes/cm. The results indicate mouse urine will not respond to capillarity within a certain temperature window of opportunity. More testing is needed to determine this window accurately.

From the force vs. immersion depth graphs used to determine surface tension, force hysteresis was apparent. Assuming everything else constant, it is concluded that this hysteresis is directly related to differences between advancing and receding contact angles. Contact angle hysteresis is a function of drop volume. With very small volumes both types of urine remained suspended when the stainless steel substrate was rotated to a vertical position. When the volume was increased five-fold, the rat urine moved with very little rotation of the substrate. However, with the same volume of mouse urine, though hysteresis was obvious, movement of the droplet was sluggish at an angle up to 45 degrees. From this observation it is expected that waste removal of the mouse in microgravity will be difficult in the direction along the wall.

The results show that the best strategy is to design removal methods through the wall the moment the urine is emitted.

11. APPENDIX A

URINE SAMPLES SENT TO NMCR

Batch #	Date Sent	Volume	Animals	Type of collection and comments
10601	January 2, 2001	N/A	6 Groups of 12 ICR strain female mice approximately 14 - 22 weeks old. Ranged from 33 - 43 grams per individual. They had never given birth. Acclimated to the NASA RFB foodbar (Teklan Diets, Madison WI) for at least one week.	Upside down Stainless steel pyramid with commercial separator - High contamination with food, feces and drinking water because of apparatus. Samples collected over 6 days each 24 hours, then frozen, then thawed and combined prior to refreezing . Packaged with insulation but would defrost within hours of the overnight delivery.
11201	January 10, 2001	ca 50 ml	2 Groups of 6 ICR mice female mice per sample 1	Maryland Plastics commercial metabolic cages - small degree of contamination. Collected each 24 hours and frozen. Daily samples added on top of frozen.
13001	January 29, 2001	ca 15 ml	At least 12 X ICR female mice acclimated to food bar - size and age as per sample 1 - Fresh collection	Expressing urine onto glass surface then used syringe to collect, transfer to vial and freeze. Combined with sliding stainless steel plate under active mice, then going "boo" to scare the pee out of them, and then using syringe to collect as above.
		ca 8 ml	12 X ICR males. All siblings obtained from our colony housed together. Age less than 8 weeks (check) at 35 - 45 grams	As per sample 3
20201	February 1, 2001	ca 40 ml	Several ICR females as per sample 1	As per sample 2
Not used	February 21, 2001	ca 50 ml	2 X 450 gram Sprague Dawley male rats - *NOTE - animals loosing weight in cages - samples not representative - John kizito notified.*	Maryland Plastics commercial metabolic cages - small degree of contamination. Collected over 24 hours and removed and frozen every 8 - 10 hours and composited.
Not used		??	2 X 450 gram Sprague Dawley male rats - *NOTE - animals loosing weight in cages - samples not representative - John kizito notified.*	As per sample 6 but collected over 8 hours and removed and frozen every 1-1.5 hours and composited.
13001	February 26, 2001	??	4 X 450 gram Sprague Dawley male rats. These rats have never bred.	As per sample 6 but collected over 8 hours and removed and frozen every 1-1.5 hours and composited.

40401	April 3, 2001	ca 15 ml	2 X 600 gram Sprague Dawley male rats. These rats have never bred. Acclimated to foodbar for several days.	As per sample 6 but collected over 8 hours and removed and frozen every 1-1.5 hours and composited. Shipped with dry ice.
	April 3, 2001	ca 15 ml	2 X 400 gram Sprague Dawley female rats. These rats have never bred. Acclimated to foodbar for several days.	As per sample 6 but collected over 8 hours and removed and frozen every 1-1.5 hours and composited. Shipped with dry ice.
	April 3, 2001	ca 15 ml	12 X ICR male mice. Acclimated to foodbar for several days. All siblings obtained from our colony housed together. Age around 13 weeks at 35 - 45 grams	Slide clean stainless steel plate under the cage and use syringe to collect urine hourly then freeze. Shipped with dry ice.
	April 3, 2001	ca 15 ml	12 X ICR Female mice aged 16 weeks weight 30 - 60 gram and acclimated to foodbar for several days	Slide clean stainless steel plate under the cage and use syringe to collect urine hourly then freeze. Shipped with dry ice.

[1] *Measurements of Rodent Urine Velocity*. Will Duiker. March 2001.
[2] Policy on Reporting Uncertainties in Experimental Measurements and Results. *ASME Journal of Heat Transfer.* **115**, 5-6 (1993).
[3] Standard Specification and Operating Instructions for Glass Capillary Kinematic Viscometers. ASTM D 446 -97$^{\epsilon}$. 197-216.
[4] Reverse-Flow Viscometers. ASTM D 2170. 196-97.
[5] Wilhelmy Method of Measuring Surface Tension. ASTM 971.